U.S. Department of Homeland Security
Washington, DC 20472

FEMA

March 26, 2008

NOTE TO FILE: File on the Mississippi Coastal Study

FROM: Emily Hirsch
Program Specialist
Engineering Management Branch

SUBJECT: FEMA review of "Wave Setup Methodology for the FEMA Mississippi Flood Study," by Donald Slinn, dated March 19, 2008.

The document, "Wave Setup Methodology for the FEMA Mississippi Flood Study," is appropriate for release by FEMA. The document provides valuable information on the analysis that was performed for the Mississippi coastal flood hazard study.

In addition to the information on the approach to wave setup for the Mississippi coastal flood study the document provides many opinions that do not necessarily represent the views of FEMA. This report should only be utilized to provide information on the technical approaches for the Mississippi coastal study.

Wave Setup Methodology for the FEMA Mississippi Flood Study

Donald Slinn
University of Florida, Gainesville, Florida

March 19, 2008
(Revised March 26, 2008)

Executive Summary

Wave setup contributes to the coastal storm surge during hurricanes. Representing two-dimensional (2-D) wave setup in storm surge models has become common practice in the Coastal Engineering community. In the FEMA study, wave fields were calculated with the Wave Action Model (WAM) in deep water and with the Simulating Waves Nearshore (SWAN) model in shallow water. The momentum transfer from the wave field to the depth integrated water column was calculated using the standard radiation stress theory. The coupled wave-surge modeling system implemented two-way coupling using an iterative method. First wave fields were calculated on low resolution grids assuming an undisturbed ocean at mean sea level using the SWAN model. Then the time dependent storm surge was calculated on a low resolution grid with the ADCIRC model to the shoreline and extrapolated onshore, forced by both wind and wave forces. These storm surge water levels were then used as the time dependent water depths and the wave fields were calculated a second time on a high resolution (160 meter) grid along the Mississippi coastline. High resolution wave forces were then used to force the high resolution ADCIRC (Advanced Circulation) model for the Mississippi Flood Study. The process was implemented for approximately 228 storm simulations to characterize the flood probabilities along the Mississippi coast using the JPM approach (Joint Probability Method). Typically the wave forces contributed approximately 0.25 to 0.75 meters to the total storm surge along the Mississippi and Louisiana coastline. The 100-year and 500-year wave heights and periods were also determined offshore from the SWAN wave simulations for use as input values for starting locations for the FEMA overland wave model WHAFIS.

1.0 Introduction

The URS Group has an Indefinite Delivery/Indefinite Quantity IDIQ contract with the Federal Emergency Management Agency (FEMA) to support the Hazard Mitigation Technical Assistance Program (HMTAP). The Mississippi Coastal Flood Hazard Project (TO-18) was assigned under this contract. The purpose of this project was to develop revised maps of the coastal flood zones as defined by the National Flood Insurance Program. The primary component of the mapping was the determination of coastal flooding hazard elevations for 10%, 2%, 1% and 0.2% chance of being equaled or exceeded along the Mississippi coast. The development of the coastal flooding hazard elevation at any location requires an estimate of the storm surge elevation and an associated wave height. The surge elevations were developed by simulating storms using

the circulation model ADCIRC. The associated inland propagation of waves was developed using the Wave Height Analysis for Flood Insurance Studies (WHAFIS).

This report documents the wave modeling conducted in support of TO-18. Wave modeling was implemented for two primary purposes:

(1) to provide estimates of the radiation stress gradients needed as input to the surge models
(2) provide estimates of offshore wave heights to support the (WHAFIS) analysis of inland wave propagation

Wave forces caused by gradients in the wave-induced radiation stresses are an important component of a typical storm surge. They create a static wave-setup that can nominally amount to as much as 10 to 15% of the measured Coastal High Water Marks (CHWMs) on the open coast and potentially more with bays and estuaries. Along the open Gulf coast the wave set-up component of the storm surge is variable in space and depends on the conditions of each individual storm. As the storm and associated surge propagate inland the spatial differences of the wave setup become more obvious. Therefore, these effects must be an integral part of each individual computed storm surge. The wave setup for each storm simulation was developed using a 2D wave model.

The WHAFIS analysis consists of propagating offshore waves that are associated with the surges inland. It is applied to discrete transects along the coastline. For each exceedance value surge elevation, the associated wave height and period is propagated inland along the transect and any modification due to vegetation, topography and obstructions are accounted for in the analysis. The same 2D wave modeling that supported the development of radiation stress gradients in the storm surge analysis was used to obtain the associated wave height and period at the offshore extent of each WHAFIS transect.

2.0 Wave Model Selection

Hurricane winds transfer momentum to the wave field and that wave momentum is transferred to the storm surge when the waves break in coastal waters. Since a hurricane is an evolving, localized, concentrated wind storm, with nearly circular wind fields, that decay with distance from the eye of the storm, the wave field never has a chance to reach any kind of equilibrium state. Thus a time-dependent wave model is necessary to capture important aspects of the wave field. The current generation of deep-water spectral wave models, such as WAM (the Wave Action Model), are skillful at predicting the evolving wave field under tropical storm and hurricane conditions. In the last 5 to 10 years, the focus of the research community has been on estimating wave fields under storm conditions in coastal and nearshore environments. This is a much more complex physical problem than deep-water wave prediction, because additional physical processes become important. In deep water, the dominant balance is between wind energy input to the wave field, radiation of wave energy away from regions of

strong winds, and transfer of wave energy between different frequency bands. In shallow water, additional processes can become equally important. These include depth limited wave breaking, loss of wave energy by bottom friction, wave refraction by topography and currents, changes in wave length due to shoaling and additional transfer of energy between wave frequencies by triad interactions that are suppressed in deeper water. All of these processes are represented in SWAN.

Implementing a two-dimensional wave model is the current state-of-the-art for including wave-setup in storm surge calculations. The two most popular open-source models available today are STWAVE (Steady State Waves) (developed by the U.S. Army Corps of Engineers ERDC) and SWAN (developed by Delft University in the Netherlands). STWAVE has the advantage of being more efficient and is adequate for most surf zone applications. SWAN has the advantages of including more physical processes including bottom friction and non-stationary physics. Recent comparisons of both models for the IPET study of Hurricane Katrina by the US Army Corps of Engineers showed that SWAN performed better during phases of wave growth. In recent work, several investigators have shown that coupling wave and surge models can significantly increase the accuracy of storm surge predictions. The wave and surge modeling system that we are implementing for the Mississippi Flood Mapping study is an improved version of the coupled modeling system developed under previous support from the National Oceanographic Partnership Program (NOAA, NSF, ONR, NASA) the Florida Department of Transportation, and the US Army Corps of Engineers.

The 2-D approach offers a very complete and state-of-the-art method that can be applied to the Mississippi Coastal Storm Surge Project. A similar approach was implemented by the FEMA Region 6, Louisiana Flood Study group. In addition, similar 2-D wave setup methods are being implemented by the US Army Corps of Engineers task force that is conducting the contemporary Mississippi Coastal Improvement Project (MisCIP) Study. In order to maintain uniformity of methodology 2-D wave setup was an important feature of the FEMA Mississippi wave study. The SWAN wave model has superior physical parameterizations of key wave dynamics, compared to the coastal wave model STWAVE that was implemented in the Army Corps group projects. Comparison of results for test problems between the models will be described below.

Both STWAVE and SWAN solve the Wave Action Balance Equation in spectral space, but they have different definitions of source and sink terms and different numerical solution procedures. SWAN is about 2000 pages long of Fortran Code and the SWAVE Fortran Code is about 50 pages long. Thus, it is simple to understand how SWAN contains many more physical parameterizations. STWAVE runs approximately five times faster. STWAVE 5.0, the currently available model, however, does not calculate unsteady wave fields, that are characteristic of hurricanes. STWAVE does not include bottom friction parameterizations. STWAVE does not calculate waves propagating in 360 degrees of a circle, it only calculates waves propagating in 170 degrees of a circle. Hurricanes, however, generate waves in all directions. STWAVE does not include wave diffraction, an important process when wave energy penetrates between an opening in barrier islands. The wave breaking model in STWAVE is not slope dependent.

STWAVE does not include wave-current refraction and it uses a simpler method to transfer energy between wave frequency bands. SWAN includes all of these physical processes. More published papers exist supporting the accuracy of SWAN. For these reasons we strongly preferred using the SWAN model. Nevertheless, since STWAVE was developed by scientists at the US Army Corps of Engineers, it was natural for them to use their own model when conducting the Corps' hurricane modeling projects and we concede that it is a rational and acceptable alternative within the requirements of the project and that the uncertainties in the accuracy of the wave models may be comparable to the differences in the results between them. When the bathymetry, wind or wave fields are two-dimensional it is advantageous to use a 2D approach.

The SWAN model includes many physical processes to obtain a realistic estimate of random wave fields. The primary input fields for SWAN are the bathymetry, the wind fields, and the wave boundary conditions. The SWAN model is a phase averaged model, for simulation of waves in shallow, intermediate or deep water. It was developed by the same group that developed the WAM model. It includes physical representations of wave attenuation due to bottom friction, shelf slope dependent depth limited breaking, unsteady wave fields development, bathymetric and current wave refraction, wave diffraction, sub-grid obstacles. Wave energy transfer from different wave frequency bands is calculated by specific triad and quadruplet wave-wave interactions. It includes sub-models for the physics of wave white-capping and steepness limited breaking as well as exponential wind-wave growth.

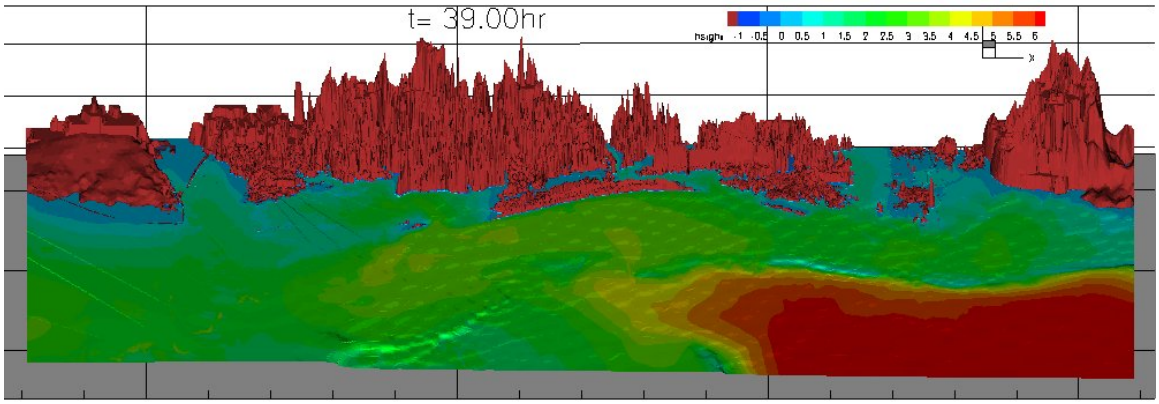

Figure 1. A visualization of the wave amplitude and flooding along the Mississippi Coast during Hurricane Katrina.

Figure 1 shows a snapshot of the wave field in the coastal domain during a simulation of hurricane Katrina near landfall. The model has been extensively calibrated and published in the open and refereed literature [See a partial list of references in Section 5.1 below]. The SWAN Fortran source code is open source code and available without charge. In our final implementation, the coupled low-resolution ADCIRC and SWAN system runs in approximately 3 days of CPU time on a single processor computer, or in about 3 hours of real time on a 32 processor computer for a 3 day hurricane simulation.

3.0 Model Configuration

Details of the FEMA-URS wave setup methodology used for this study are described here. SWAN requires (1) bathymetry, (2) boundary conditions, (3) wind fields, and (4) a grid system and the specification of some numerical parameters. Each of these is described below.

3.1 Bathymetry Data

The ocean bathymetry and coastal topography, shown in Figures 2 and 3, were taken from two sources, the National Geophysical Data Center (NGDC) and from the URS ADCIRC Grid, which incorporated the high resolution Lidar survey data. In the coastal zone the bathymetry in the wave models was interpolated from the URS ADCIRC Grid. The reference level was NAVD88. There were two bathymetries implemented for different tests. A pre-Katrina grid, that was used to run two of the calibration storms, *i.e.*, Betsy and Camille, and a post-Katrina grid. In deep water, the wave field is relatively insensitive to the bathymetry. If the water is deeper than about 200 meters then the waves are not influenced by the water depth. Figure 2 shows the bathymetry in the North Atlantic and Gulf of Mexico domain that was used for the deep water Wave Action Model (WAM) and the low resolution ADCIRC grid to obtain estimates of the preliminary water levels.

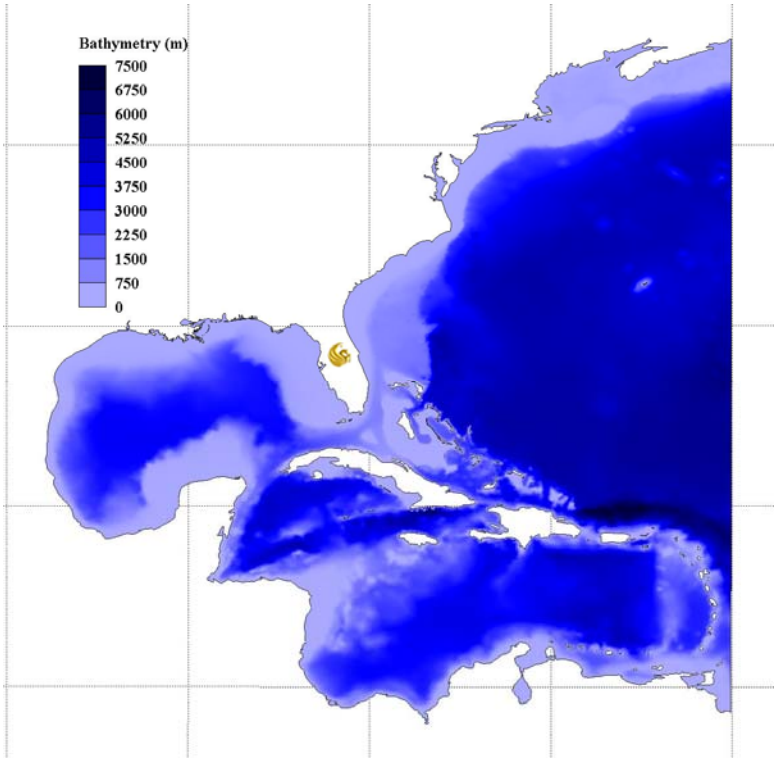

Figure 2. Bathymetry from the ADCIRC model used in the low resolution ADCIRC grid and for the regional wave model WAM that covers the Gulf of Mexico, shown in Figure 4 below.

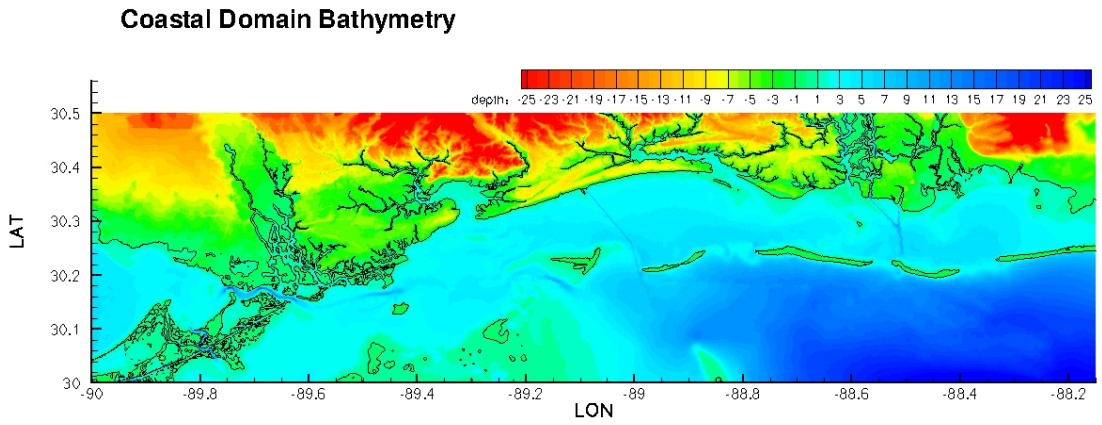

Figure 3. Post-Katrina coastal bathymetry used in the wave model developed from URS and NGDC data sets.

3.2 Wind Field Data

Wind fields from Ocean Weather Inc. (OWI) were used to drive the surge and wave models. These are the same wind fields used to force the ADCIRC circulation model. Documentation of the wind fields and their independent QA/QC review can be found in the main engineering report.

3.3 Boundary Conditions Data: (WAM)

Deep water waves were calculated using the WAM-3G (Third Generation Wave Action Model; Komen et al., 1994), implemented by Ocean Weather Inc. (OWI). They provided wave spectra on the regional wave boundaries described below. The wave spectra were given in 15 degree directional bins and for 26 frequencies at 15 minute time intervals over the course of (usually) three-day long hurricanes. The basin wave field was calculated on a 10 km grid (0.1 degree). These wave spectra were interpolated in spectral density space onto our higher resolution wave grids (5 degree directional spectra) and higher resolution spatial coverage.

3.4 Nested Grid System

We implemented the model on a Cartesian coordinate system, but it also can be implemented on spherical or curvilinear grids. The SWAN model was implemented on a set of nested grids, with resolutions ranging from 2.5 km down to approximately 160 meters. This nesting system was designed to optimize grid resolution and simulation time. Three levels of wave grids were used, and are shown in Figure 4. At the coarsest resolution, there was a basin grid that covered the entire Gulf of Mexico with grid resolution of 0.1 degrees or approximately 10 km. It is pictured in the left panel of Figure 4. Inset in this left panel is the second grid level (the red box in the left panel is the second grid level, and it is blown up in the right panel). This is the Louisiana-

Mississippi region grid, where we implemented a grid resolution of 2.5 km. The Basin Grid is shown in the left panel of Figure 4, with the location of the Region grid shown in this panel by the red box. The Region grid is also shown in the right panel of Figure 4, with the location of the Coastal Grids shown in the alternating red and black boxes. And in the coastal Mississippi region we implemented 9 coastal grids, that overlapped along the coast with 160 meter grid spacing in the x direction, and 180 meter grid spacing in the y direction (both are 0.00166667 degrees at this latitude). The coastal zone was divided into 9 grids in order to run faster on the computers. Each grid had 301 x 151 grid points and extended approximately 54 km in the offshore direction and 24 km in the alongshore direction. The coastal grids, shown in the inset in the right panel of Figure 4, overlapped by 2.4 kilometers on either side, and the results of in the overlapping region were blended by weighting the solution closest to its interior domain from one to zero, linearly depending on it's distance from the interior of the domain.

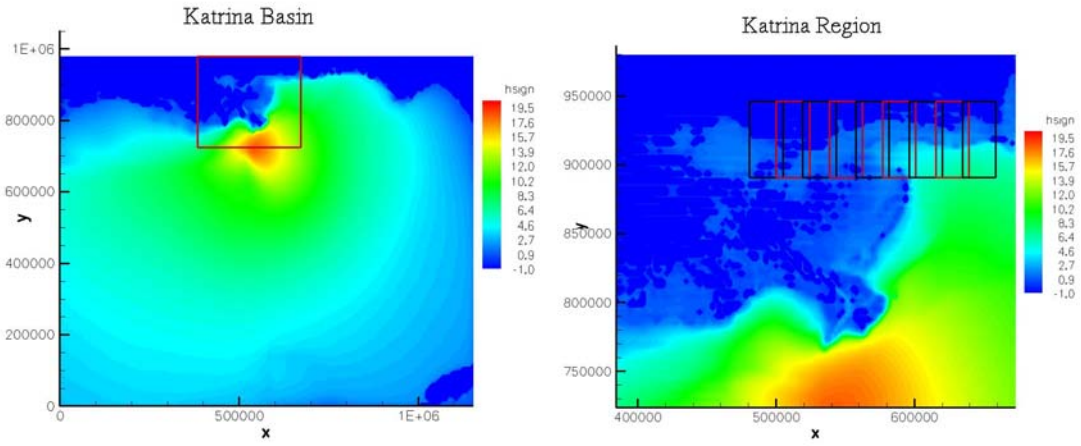

Figure 4. Computational Domains used in the wave setup modeling approach. The left panel shows the Gulf of Mexico grid region. The right panel is a blow up of the red square from the left panel. It includes the Louisiana, Mississippi and Alabama coast lines. The right panel also includes the location and overlapping regions of the 9 coastal grids.

3.5 SWAN Numerical Model Parameters

SWAN model version 40.51 was used for this study. It was implemented with 72 directional bins (e.g., with 5 degree directional wave spectral bins) and with 26 frequency bins (from 0.0314 to 0.4177 Hz) covering wave periods between approximately 32 seconds to down to 1 second (the last frequency bin for the highest frequency waves is nominally at 2.4 second periods, but represents waves with periods from 0.0 to 2.4 seconds The time step was 15 minutes and the model data was output every 30 minutes.

4.0 Basic Wave Setup Modeling System Algorithm

The interaction of a storm surge and wave generation is a highly coupled process. The wave heights and periods depend on the surge height (i.e., water depth) and the surge height depends on the radiation stress gradients, which are dependent on the water depth. Ideally, a fully coupled model simultaneously including surge and wave simulations could be used. However, there is no model currently available for applications in this study and therefore an iterative approach using separate surge models and wave models has been employed. We note that we appropriately restrict our attention here to the static, or time averaged, wave setup. There is a second component of the wave setup, called the dynamic setup, associated with different wave packets. Larger wave groups, may last for a few minutes, and cause larger waves setup for a short duration, these are followed by smaller wave groups, that would have less associated wave setup. Our averaging time interval is 15 minutes, and we drive our wave model with 30 minute averaged winds, and therefore we will produce the average wave setup, from the average wave fields, rather than a possible maximum wave setup that might occur on a shorter time interval.

4.1 Description of Algorithm

The overall iterative scheme for the method involves rapidly computing a sequence of water levels along the whole coast and calculating the coastal wave field and offshore into Mississippi Sound in a reasonably rapid fashion. This is done for each storm to be simulated by using the ADCIRC model on a relatively low resolution grid. This existing model is set-up for the Mississippi coast using a grid with about 58,000 nodes. It does not provide for overland propagation of the surge These output files are then to be input to a 2-D wave propagation and breaking model (SWAN). This results in outputting files with the radiation stress gradients for each grid point in the high resolution ADCIRC grid at 30 minute time intervals. The file containing the radiation stress field is then input to the detailed ADCIRC grid (900,450 nodes) that does provide for overland propagation of the surge. This detailed model has much more stringent computational requirements and runs more slowly than the other two models (58K ADCIRC and SWAN) that are to be used for each storm. This difference in computational requirements means that the scheme to prepare the radiation stress gradient input files can be implemented faster than the runs of the detailed ADCIRC model. In other words, the project schedule could be maintained because the more computationally intensive model sets the overall rate of progress.

The wind, wave and surge models are linked at many levels. First the wave model SWAN is run, forced with the hurricane winds, assuming no surge is present on the Basin (Gulf of Mexico) and Regional (Louisiana to Alabama) domains. Second, a coarse resolution (58,000 element ADCIRC grid) of the Gulf of Mexico is run forced with both the wind and preliminary wave fields to estimate the water elevations. Third, the SWAN model is run on 10 Coastal Mississippi grids with high resolution (approximately 160 meters). The main difference in the second implementation of the wave model is that the water elevations from the low resolution ADCIRC grid are included in the total water elevations. The wave fields are also calculated over the

flooded land regions, assuming that the flood levels are able to achieve a hydrostatic balance in the inland areas. The wave fields from the 10 grids are then reassembled and the wave forces that act on the water column are then calculated and interpolated onto the high resolution (900,450 elements) ADCIRC grid for the coastal flooding studies. An advantage of this methodology is that the wave forces that produce set-up are not overestimated. They are spatially and temporally varying using the best state-of-the-science methodologies. The computational cost is relatively small to add the wave components, compared to the cost of calculating the total storm surge. The only inputs required for the coupled modeling system are the time and spatially varying wind fields and the bathymetry. The more accurate the wind fields, the more accurate the resulting total surge and set-up predictions. In previous implementations of this methodology, the OWI and H-Wind (a NOAA Wind product) wind fields have been used with considerable success by the IPET (Interagency Performance Evaluation Taskforce) and NOPP (National Oceanographic Partnership Program) teams. The 2-D wave setup methodology has been implemented in a nearly equivalent manner recently by the US Army Corps of Engineers team led by Dr. Joannes Westerink for the IPET and FEMA Region VI studies. The URS team has also adopted the OWI wind fields as their model input.

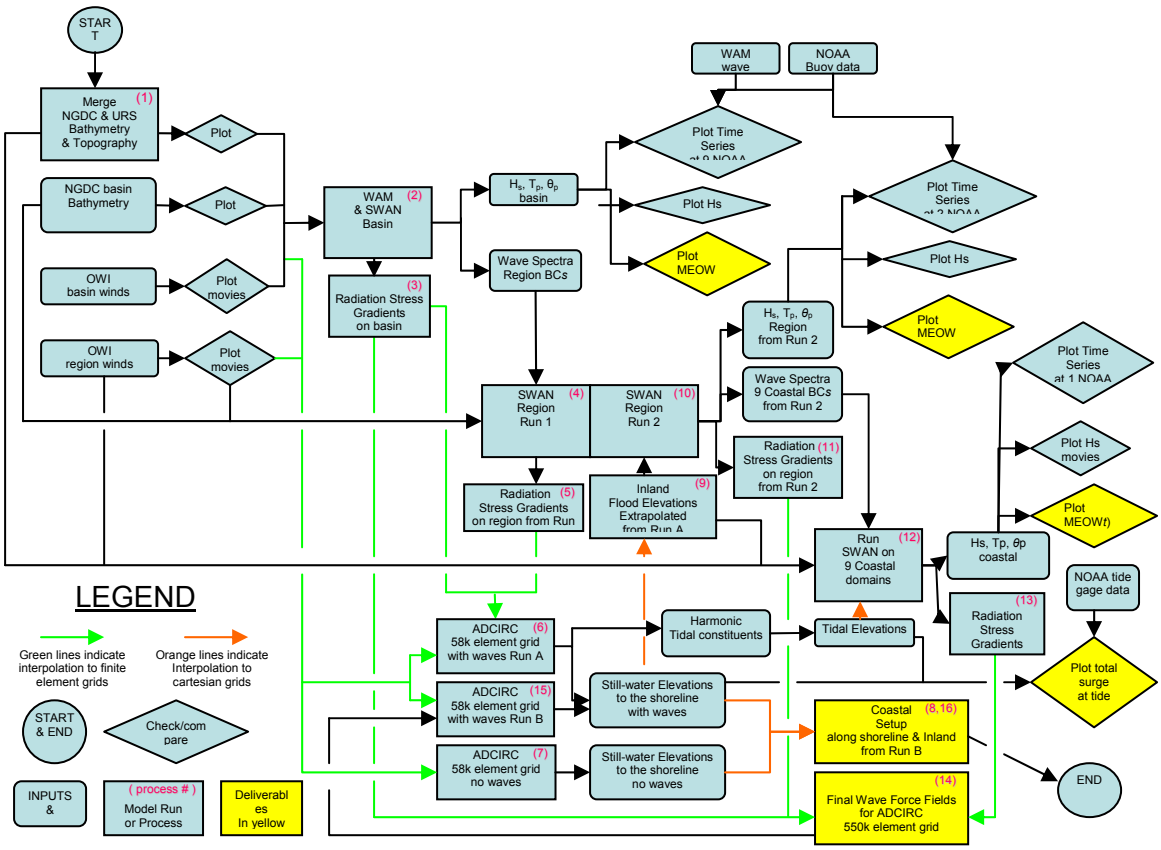

Figure 5. Flow chart of Wave Setup Methodology.

Figure 5 shows a flow chart of the wave setup methodology. It has 16 major steps.

1. Merge NGDC and URS bathymetries.
2. Run WAM for the Basin. Interpolate the wave boundary conditions for the region grid.
3. Calculate radiation stress gradients on the basin. (optional)
4. Run SWAN on the Region.
5. Calculate radiation stress gradients on the region.
6. Run ADCIRC on the 58K element grid with wave forces from 3 and 5 above.
7. Run ADCIRC with the 58K element grid with no wave forces (optional step used in development.)
8. Calculate coastal Wave Surge on Shoreline and Inland.
9. Extrapolate the coastal water levels inland horizontally using a hydrostatic approximation.
10. Run SWAN again on the Region grid with flood levels active.
11. Calculate the radiation stress gradients on the regions grid.
12. Run SWAN on the 9 coastal domains.
13. Calculate the radiation stress gradients on the merged coastal and region grids.
14. Interpolate the final wave force fields onto the 900,450 element ADCIRC grid, making a fort.23 forcing file.
15. Rerun the low resolution ADCIRC grid if desired (optional).
16. Determine coastal setup along shoreline on low resolution grid (optional).

An additional step in the process is to decrease the magnitude of the wave forces in vegetated areas. This methodology follows the analysis of Dean and Bender (2005) that showed that wave attenuation in vegetated areas should not be all attributed to transfer of momentum from the waves to the water column. Frictional losses to the trees or bushes could decrease the radiation stress gradients by 1/3 depending on the relative water depths to the height of the vegetation.

The modeling system has been completely automated using shell scripting language and is operable on any Unix platform. We implemented on a 1,000 processor Department of Energy IBM Supercomputer and on a suite of single and dual processor Linux workstations. The system is nearly platform independent. It compiles all of the open source models locally on the computers, including SWAN and ADCIRC, and all of the 20 or so interfacing programs that are written in Fortran. The only changes necessary on a new platform are related to the necessary compiler flags and batch submission system to submit the simulations to the main CPU. Typical production on the DOE system were approximately 5 simulations per day. On the system of 12 CPU's dedicated to this project the production rate was approximately 4 simulations per day.

4.2 Example Implementation of the Algorithm

In this section we show an example of results from an implementation of the wave modeling system for the case of Hurricane Katrina. First we show sample results of the wave field on the basin grid (the Gulf of Mexico), then results on the region grid (Louisiana to Alabama) and then results on the high resolution, coastal Mississippi grids. An illustration of how the wave fields would differ if two-way coupling was not implemented is also presented.

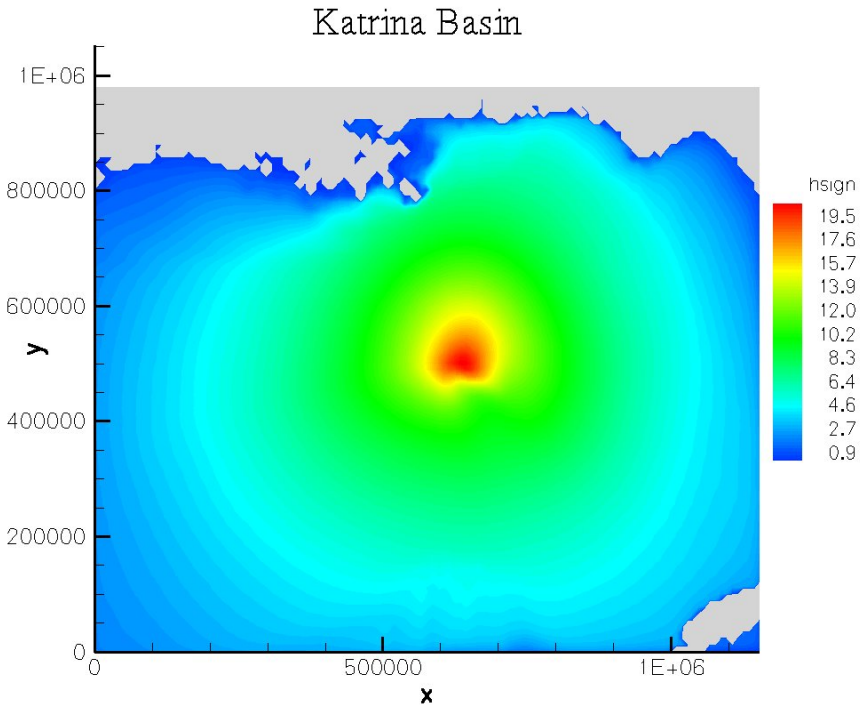

Figure 6. Significant Wave Heights predicted during Hurricane Katrina in the Basin Scale grid.

Figure 6 shows the spatial distribution of a snap shot in time of the significant wave heights during Hurricane Katrina. The significant wave height, H_s, is the average height of the 1/3 largest waves representative of the spectrum, or more exactly this is also called H_{m0} the zeroth moment of the wave energy density spectrum. The waves propagate away from the center of the storm faster than the winds do and reach the shore before the strong winds of a hurricane arrive, often causing significant wave setup prior to the landfall of the storm. Wave heights of approximately 21 meters were predicted near the eye of the hurricane.

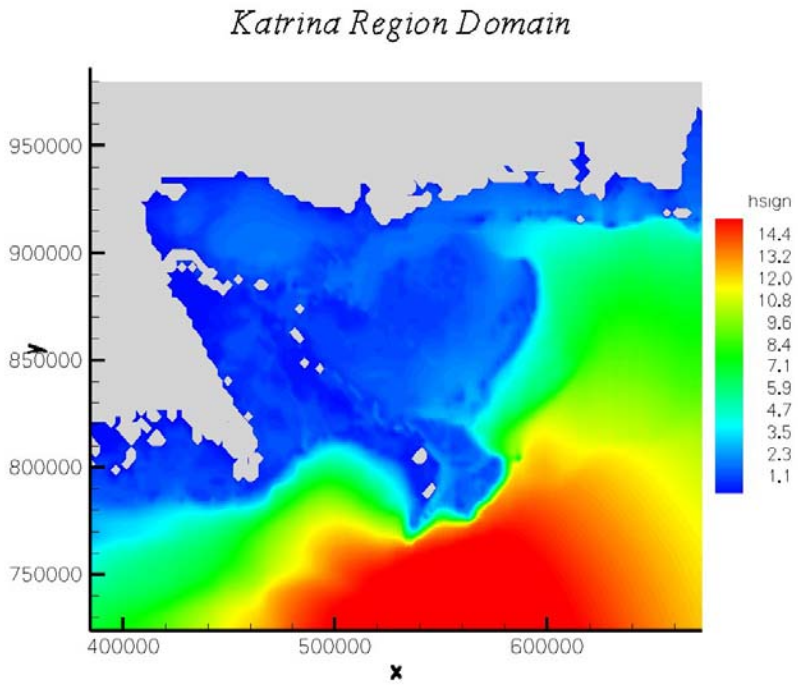

Figure 7. Coastal Region Wave Grid and Bathymetry.

Figure 7 shows wave model results on the Region domain near the peak of Hurricane Katrina. This grid has 2.5 km grid resolution. The largest waves occur outside of the barrier islands. The low lying topography is flooded with water during the course of the simulation. This simulation is used predominantly to feed accurate boundary conditions to the nested high resolution grids shown in Figure 8. Figure 8 has two panels. In the top panel the significant wave heights are shown as calculated during step 12 of the modeling system that includes coastal flooding and model coupling with ADCIRC. The bottom panel shows the wave forces (radiation stress gradients) calculated in the coastal domain (step 13 in the modeling system described above.) We note for completeness that in an extensive study conducted previously for the Florida Department of Transportation, we showed that there is generally less than a 1 percent change of the wave and water fields that would result if a third iteration of wave and flood coupling is conducted (Sheppard, Slinn and Hagen, 2007) and therefore it was unnecessary to include any additional iterations for the present FEMA-URS study.

The top panel of Figure 8 shows the peak wave heights in meters (top panel) and wave forces transferred to the water column (bottom panel) in the merged coastal domains from a simulation. The units for the wave force are m^2/s^2, which is stress, N/m^2, divided by the density of water, which is the units that ADCIRC requires for it's wave forcing input files, (fort.23). These figures are typical of results from all of the production runs. The peak wave forces occur outside the barrier islands. There are strong two-dimensional effects to both the wave fields and the wave forces. There are two major surf zones. The one just outside the barrier islands is about 2 kilometers wide, and is well resolved in both the wave model (with about 15 grid points) and in the storm surge model grid, which has approximately 80 meter grid resolution there. This was

found to be an important consideration. The surf zone needs to be resolved by approximately 10 grid points, in order to conserve the momentum transfer between the wave and surge fields. The second surf zone, of course,

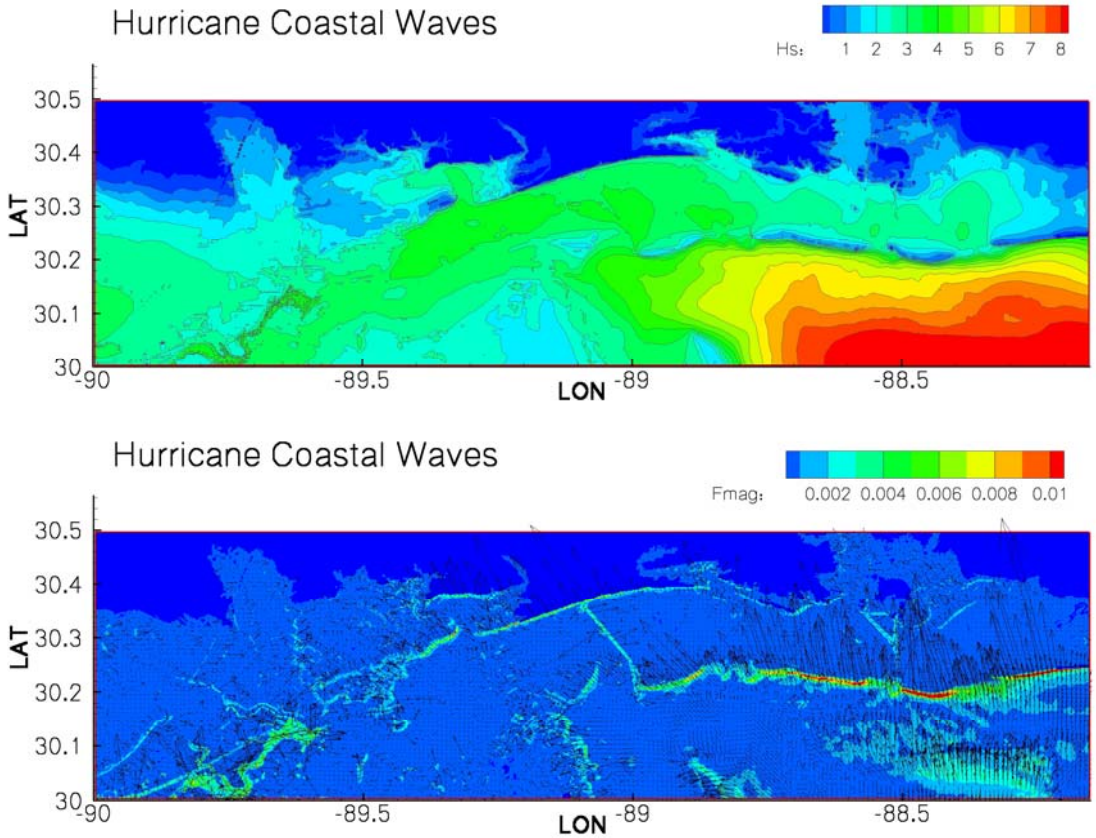

Figure 8. Top Panel: Wave heights in the coastal domain from the SWAN simulations for Hurricane Katrina. Bottom Panel: Maximum values of the Wave Forces in the coastal domain during the Katrina simulation in the merged coastal domains.

occurs in the immediate vicinity of the shore line. Other regions of strong variability are evident in the wave force plot. Some of these are caused by dredged shipping channels that are much deeper than the surrounding bathymetry. The deeper water allows much larger waves to propagate and develop and as these diffract into shallower water, they cause breaking and transfer momentum to the depth averaged water column. Waves penetrate through the channels between the barrier islands and then diffract and spread out their energy through the channels. Waves of approximately 15 meters are predicted outside of the barrier islands. The waves reform in Mississippi Bay, between the islands and shore, over a distance of approximately 15 km. These waves are both fetch limited and depth limited, and typically have significant wave heights under 4 meters.

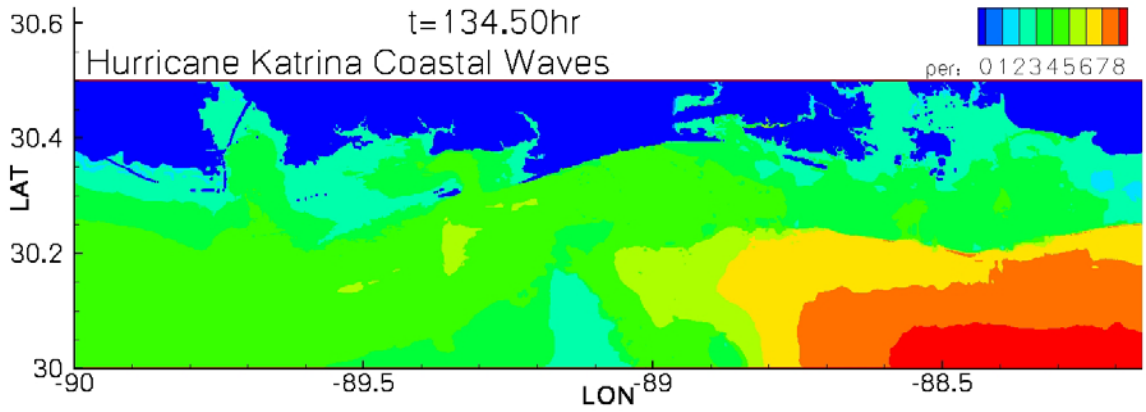

Figure 9. Snap shot of the peak wave periods T_p during Hurricane Katrina.

Figure 9 shows a snap shot in time of the peak wave periods T_p predicted from SWAN during a simulation of Hurricane Katrina. The longest wave periods, in excess of 10 seconds are generally restricted to outside of the barrier islands, the waves reform inside the barrier islands, and even during overtopping of the islands (as occurred at this time), there is little penetration of the long period waves across the shallow water over the barrier islands. Wave spectra inside Mississippi sound with more energy – frequency information content are shown in a following section.

5.0 Model Calibration and Validation

Three methods were used for model validation. First, an appeal to the scientific literature was made. Second, a couple of historical hurricanes in our area were simulated where data was available at various buoys to indicate the level of agreement with measurements. Third, comparisons were made between the two similar spectral, phase-averaged, two-dimensional coastal wave models, SWAN and STWAVE, and those results were compared to a sophisticated one-dimensional model that has been previously calibrated against hurricane wave data

5.1 Refereed SWAN Publications

There is an extensive body of literature indicating that both WAM and SWAN are state of the art models for predicting waves accurately in coastal waters. A reference list of 28 recent articles is included below that used the SWAN model and demonstrated it's capabilities and agreement with theory, lab measurements, and field data under a wide variety of circumstances:

1. Holthuijsen, L.H., N. Booij and R.C. Ris, 1993, A spectral wave model for the coastal zone, Proceedings 2nd International Symposium on Ocean Wave Measurement and Analysis, New Orleans, Louisiana, July 25-28, 1993, New York, pp. 630-641.

2. Ris, R.C., L.H. Holthuijsen and N. Booij, 1994, A spectral model for waves in the near shore zone, Proc. 24th Int. Conf. Coastal Engng, Kobe, Oct. 1994, Japan, pp. 68-78.

3. Booij, N., Holthuijsen, L.H. and R.C. Ris, 1996, The SWAN wave model for shallow water, Proc. 25th Int. Conf. Coastal Engng., Orlando, USA, Vol. 1, pp. 668-676.

4. Ris, R.C. and L.H. Holthuijsen, 1996, Spectral Modelling of current induced wave-blocking, Proc. 25th Int. Conf. Coastal Engng., Orlando, USA, Vol. 1, pp. 1247-1254.

5. Ris, R.C., 1997, Spectral Modelling of Wind Waves in Coastal Areas (Ph.D. Dissertation Delft University of Technology), Communications on Hydraulic and Geotechnical Engineering, Report No. 97-4, Delft.

6. Ris, R.C. and L.H. Holthuijsen, 1997, Modelling of current induced wave-blocking in a spectral wave model, 8th International Biennal Conference on Physics of Estuaries and Coastal Seas, J. Dronkers and M.B.A.M. Scheffers (eds.), The Hague, 139-144.

7. Holthuijsen, L.H., N. Booij and R. Padilla-Hernandez, 1997, A curvi-linear, third-generation coastal wave model, Conf. Coastal Dynamics '97, Plymouth, 128-136.

8. Booij, N., L.H. Holthuijsen, N. Doorn and A.T.M.M. Kieftenburg, 1997, Diffraction in a spectral wave model, Proceedings 3rd International Symposium on Ocean Wave Measurement and Analysis, WAVES'97, ASCE, 243-255.

9. Booij, N., L.H. Holthuijsen and R. Padilla-Hernandez, 1997, Numerical wave propagation on a curcilinear grid, Proceedings 3rd International Symposium on Ocean Wave Measurement and Analysis, WAVES'97, ASCE, 286-294.

10. Holthuijsen, L.H., N. Booij, R.C. Ris, J.H. Andorka Gal and J.C.M. de Jong, 1997, A verification of the third-generation wave model "SWAN" along the southern North Sea coast, Proceedings 3rd International Symposium on Ocean Wave Measurement and Analysis, WAVES'97, ASCE, 49-63.

11. Padilla-Hernandez, R., J. Monbaliu and L.H. Holthuijsen, 1998, Intercomparing third-generation wave model nesting, 5th International Workshop on Wave Hindcasting and Forecasting, Jan. 27-30, 1998, Melbourne, Florida, 102-112.

12. Booij, N., L.H. Holthuijsen and IJ.G. Haagsma, 1998, Comparing the second-generation HISWA wave model with the third-generation SWAN wave model, 5th International Workshop on Wave Hindcasting and Forecasting, Jan. 27-30, 1998, Melbourne, Florida, 215-222.

13. Holthuijsen, L.H., R.C. Ris and N. Booij, 1998, A verification of the third-generation wave model SWAN, 5th International Workshop on Wave Hindcasting and Forecasting, Jan. 27-30, 1998, Melbourne, Florida, 223-230.

14. Holthuijsen, L.H. and L. Cavaleri, 1998, Activities of the WISE group, 5th International Workshop on Wave Hindcasting and Forecasting, Jan. 27-30, 1998, Melbourne, Florida, 433-437.

15. Andorka Gal, J.H., L.H. Holthuijsen, J.C.M. de Jong and A.T.M.M. Kieftenburg, 1998, Wave transformation near a quasi-1D coast, 26th Int. Conf. Coastal Engng., Copenhagen,150-160

16. Holthuijsen, L.H., N. Booij and IJ.G. Haagsma, 1998, Comparing 1st-, 2nd - and 3rd-generation coastal wave modelling, 26th Int. Conf. Coastal Engng., Copenhagen, 140-149

17. Cavaleri, L. and L.H. Holthuijsen, 1998, Wave modelling in the WISE group, Proc. 26th Int. Conf. Coastal Engng., Copenhagen, 498-508

18. Booij, N. L.H. Holthuijsen and R.C. Ris, 1998, Shallow water wave modelling, Oceanology International 98, The Global Ocean, Brighton, Conference Proceedings, 3, 483-491.

19. Holthuijsen, L.H., 1998, The concept and features of the ocean wave spectrum, Provision and engineering/operational application of ocean wave spectra, COST Conference, UNESCO, 21-25 Sept., 1998, Paris, keynote address, in press.

20. Gorman, R.M. and C.G. Neilson, 1999, Modelling shallow water wave generation and transformation in an intertidal estuary, Coastal Engineering, 36, 197-217

21. Booij, N., R.C. Ris and L.H. Holthuijsen, 1999, A third-generation wave model for coastal regions, Part I, Model description and validation, J.Geoph.Research C4, 104, 7649-7666.

22. Ris, R.C., N. Booij and L.H. Holthuijsen, 1999, A third-generation wave model for coastal regions, Part II, Verification, J.Geoph.Research C4, 104, 7667-7681.

23. Padilla-Hernandez, R. and J. Monbaliu, 2001, Energy balance of wind waves as a function of the bottom friction formulation, Coastal Engineering, 43, 131-148.

24. Rogers, W.E., P.A. Hwang and D.W. Wang, 2003, Investigation of wave growth and decay in the SWAN model: three regional-scale applications, J. Phys. Oceanogr., 33, 366-389.

25. Holthuijsen, L.H., A. Herman and N. Booij, 2003, Phase-decoupled refraction-diffraction for spectral wave models, Coastal Engineering, 49, 291-305.

26. Hsu, T.-W., S.-H. Ou and J.-M. Liau, 2005, Hindcasting nearshore wind waves using a FEM code for SWAN, Coastal Engineering, 52, 177-195.

27. Zijlema, M. and A.J. van der Westhuysen, 2005, On convergence behaviour and numerical accuracy in stationary SWAN simulations of nearshore wind wave spectra, Coastal Engineering, 52, 237-256.

28. Van der Westhuysen, A.J., M. Zijlema and J.A. Battjes, 2007, Nonlinear saturation-based whitecapping dissipation in SWAN for deep and shallow water, Coastal Engineering, 54, 151-170.

5.2 Comparison to Storm Wave Buoys

The National Oceanographic and Atmospheric Administration (NOAA) maintains a number of wave buoys in the Gulf of Mexico and the information is available on line at the National Data Buoy Center web site (NDBC). The locations of several of these buoys are indicated in Figure 10.

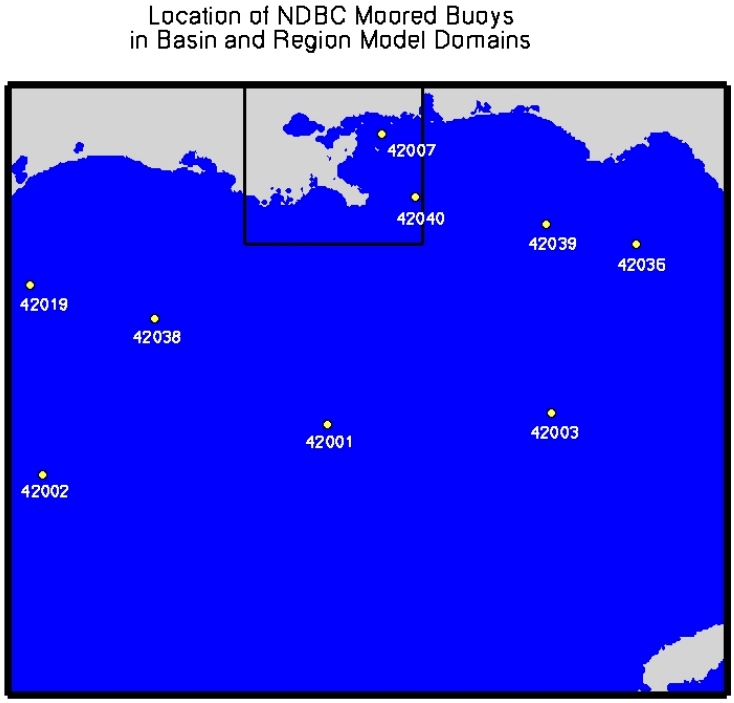

Figure 10. Location of NOAA Wave Buoys in the Gulf of Mexico.

Two of the buoys are in our region of primary interest, and all of the buoys were used for comparisons with model predictions for Hurricanes Georges (1998) and Katrina (2005). Very good agreement has been found between the OWI deep water wave model and the deep water wave buoys, and they have calibrated/verified that model against every hurricane possible throughout recorded history over the last 20 years of practicing hurricane modeling for offshore oil platforms. Buoy 42007 is of primary interest because it is located in shallow water just outside of the barrier islands in our high resolution Coastal domains. Buoy 42040 is also in our Regional domain, located outside of the barrier island chain. Figures 11 and 12 show the agreement between the model predictions and the NDBC buoys during Hurricane Katrina. Note that two of the buoys, 42003 and 42007, both broke during the peak of the storm, and so further model validation can not be obtained. The agreement, however was very good until the buoys failed. Only buoy 42040 gives disappointing agreement during Katrina. The peak measured wave heights were approximately 17 meters at this buoy, but the models, both WAM and SWAN only predicted about 12 or 13 meters.

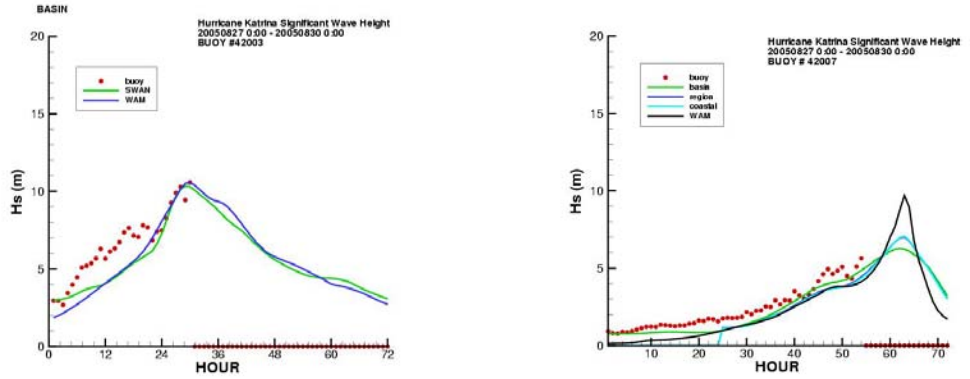

Figure 11. Comparison to Wave buoy results during Hurricane Katrina at Buoys 42003 and 42007.

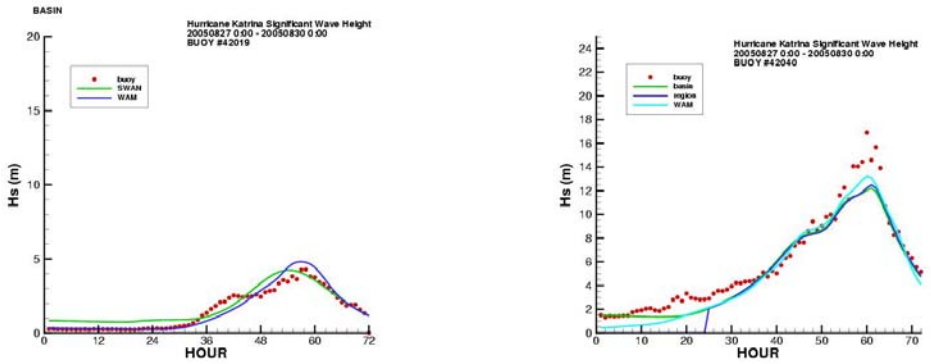

Figure 12. Comparison of wave model and buoy data during Katrina at buoys 42019 and 42040.

Figures 13 and 14 show similar results for Hurricane Georges, the largest hurricane of 1998. For this hurricane, all 4 buoys survived the storm. And favorable agreement was obtained between the model predictions and the buoy data at all of the buoys. Here, agreement with buoy 42040 was much better. There are several possible explanations as to why the Georges simulation faired better at buoy 42040 than the Katrina simulation. We offer two that are likely. First, the wave predictions are only as accurate as the wind fields that were used. They have some margin of uncertainty. However, the more logical explanation is that the eye of the storm passed nearly directly over this buoy location for Hurricane Georges, where the wave height agreement was excellent, but for Hurricane Katrina, this buoy was on the edge of and in the vicinity of steep gradients of the hurricane's strongest winds.

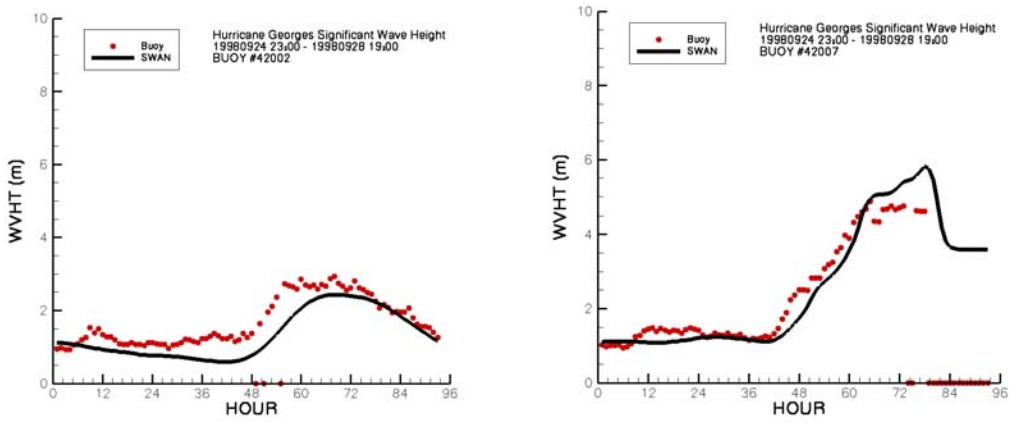

Figure 13. Comparison to Wave buoy results during Hurricane Georges (1998) at Buoys 42003 and 42007.

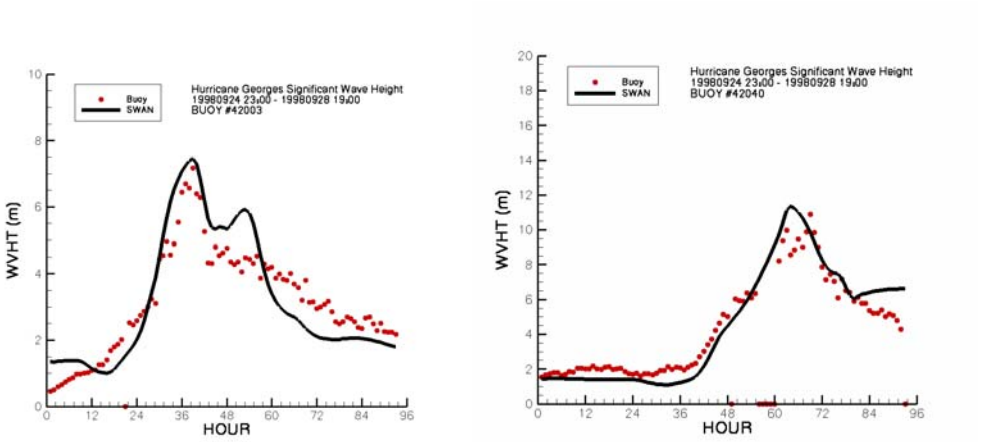

Figure 14. Comparison of wave model and buoy data during Hurricane Georges at buoys 42019 and 42040.

Maximum significant wave heights of over 21 meters during Katrina were predicted by the WAM and SWAN models at locations other than those measured at the buoys. The swath of the peak observed significant wave heights for hurricanes Katrina and Georges are shown in Figure 15. This clearly indicates that the eye of the storm passed directly over buoy 42040 for Georges but passed to the west for Katrina. Sensitivities of wave propagation or small differences between the modeled wind field on the edge of the storm could easily account for the model-data discrepancies at 42040 for Katrina.

We note that no surf zone wave gages were available for comparison to the SWAN results for the hurricanes.

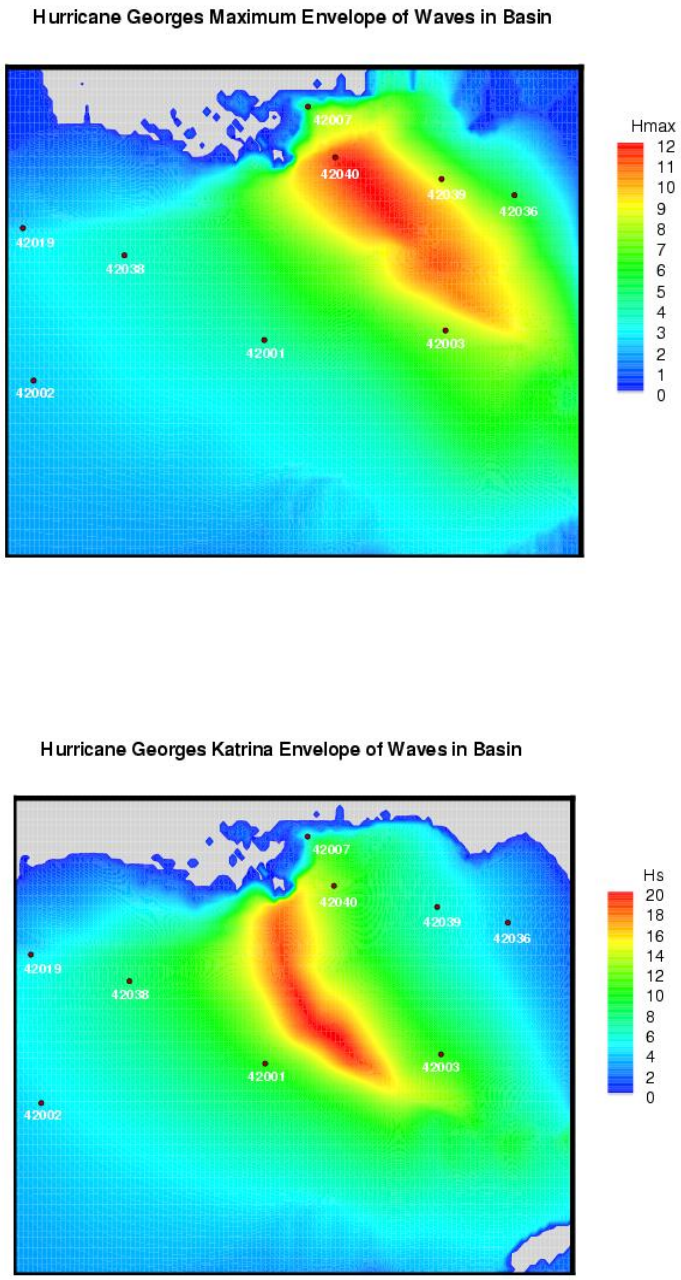

Figure 15. Maximum significant wave heights during Hurricane Katrina (top panel) and Hurricane Georges (bottom panel) during the simulations in the Basin model domains.

5.3 Comparison of SWAN model results to STWAVE and Dean's 1D model

We conducted some simple comparisons between SWAN, STWAVE and a one-dimensional wave model to understand the differences and similarities in the response of the models. The tests conducted here used steady wind fields because that is all that STWAVE is capable of examining.

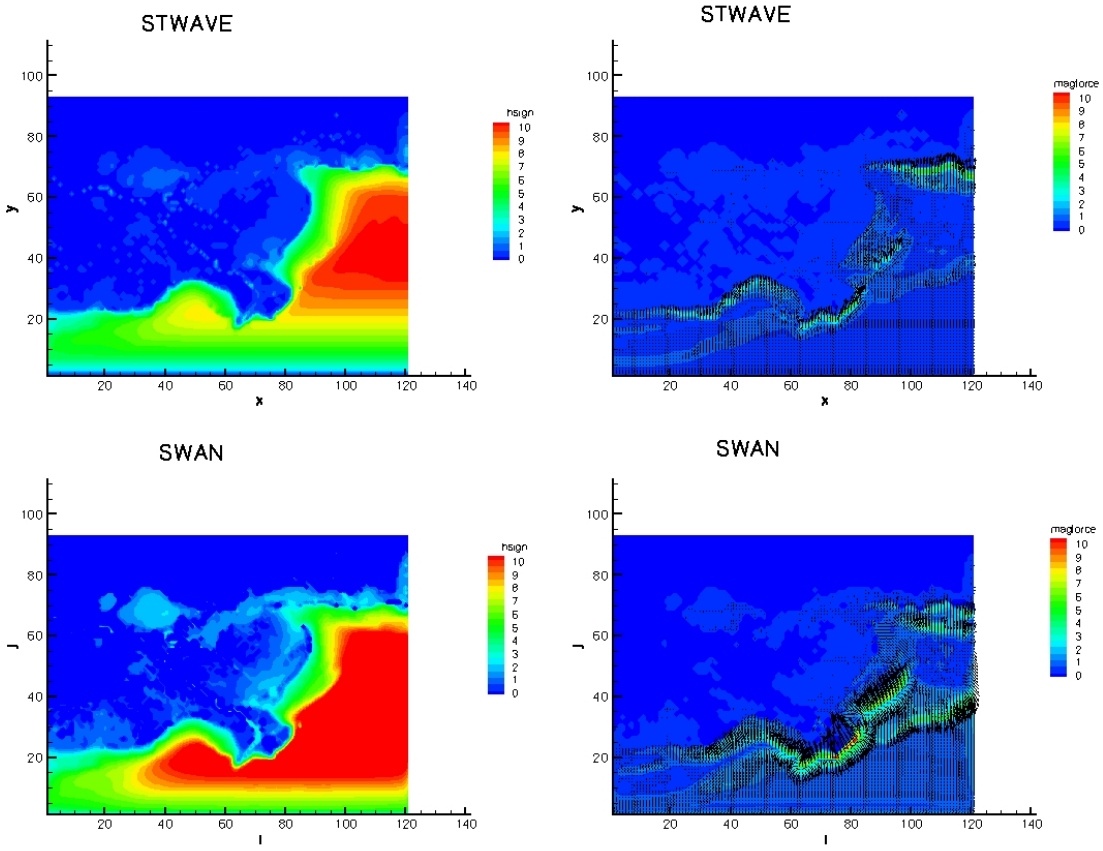

Figure 16. Comparison of results from STWAVE and SWAN for steady 50 m/s south wind. The units of the Significant Wave Heights are in meters, and the units of the force are in Pascals, the ordinate and abscissa are shown in the grid index.

Figure 16 shows a comparison of wave fields and wave forces obtained by a steady 50 m/s wind blowing from the south on the Mississippi – Louisiana coastal region with SWAN and STWAVE. In SWAN the waves grow faster and become larger. There are many similarities between the basic wave fields. The shelf regions are dominated by depth limited breaking, and the model results are similar in those regions. One striking difference is evident from the force vectors. The wind is blowing due north, and STWAVE gives almost all of the force vectors oriented due north. SWAN has a more significant refraction – diffraction model and in the coastal zones, and regions near the barrier islands and at the shore where refraction is more important, this trend is evident.

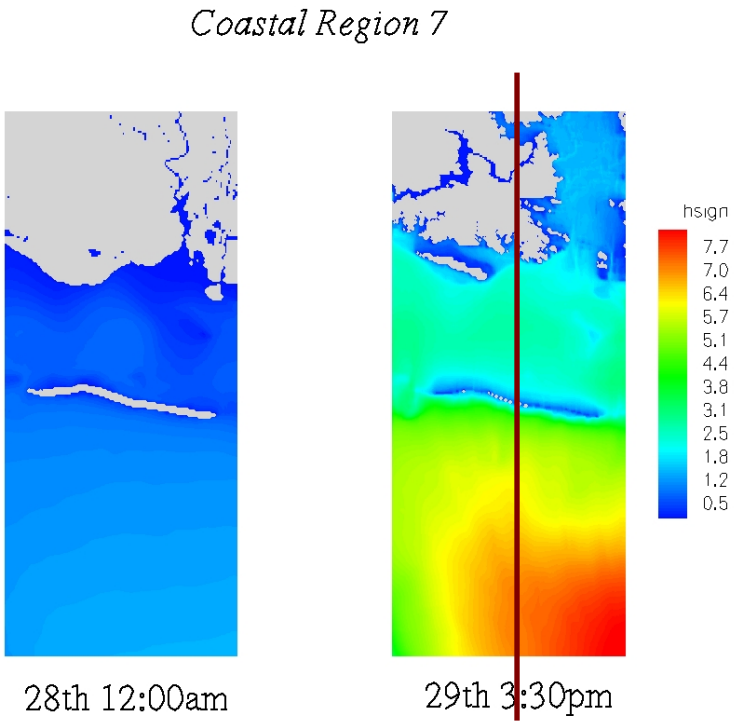

Figure 17. Location of 1-D transects for SWAN – STWAVE comparisons in the middle of Coastal Zone 7 crossing the barrier island.

We designed a simple test to examine both the wave model properties as well as the wave induced setup produced by the models. We took a 1-D transect of the bathymetry along the Mississippi shelf as indicated in Figure 17 (right panel, centerline). The bathymetry is plotted in the top panel of Figure 18.

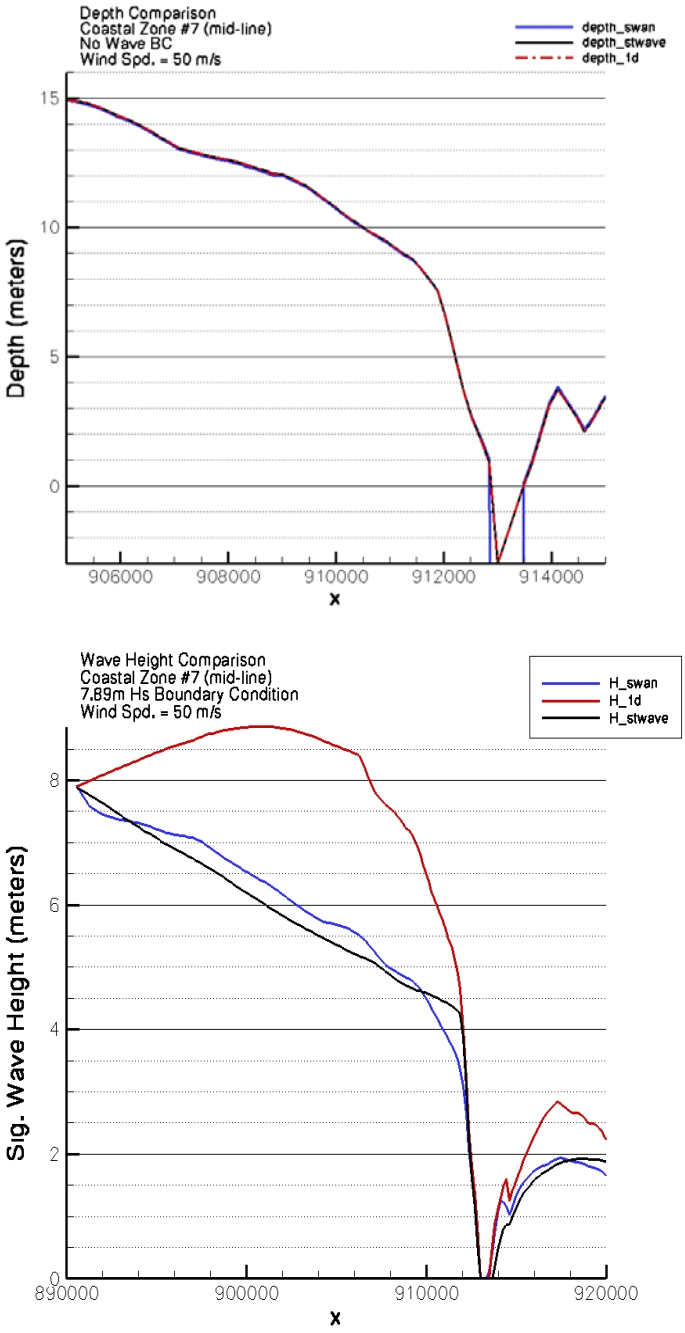

Figure 18. Case 1. 1D versions of SWAN and STWAVE comparisons. Dean's 1D model results also shown.

The water depth is approximately 15 meters at the offshore boundary, the x axis is given in meters, with the offshore boundary located at approximately 890,500 meters and the barrier islands located at about 913,000 meters, or about 12.5 km shoreward of the offshore boundary. This analysis focuses on the wave transformation and setup seaward of the barrier islands. There is another region, of course, located landward of the barrier islands, and shown in the figures from approximately x = 914,000 to 920,000 m,

representing the Mississippi Sound sheltered waters. In these simulations, no overtopping of the islands by flooding was allowed, therefore, the two sections of water are completely independent basins, and we restrict our attention to the offshore region outside of the barrier islands. We conducted three separate tests after setting up 1-D versions of STWAVE and SWAN, that had this cross-shore bathymetry profile, uniform in the along shore direction. We compared the results also to a1-D model that has been calibrated previously against hurricane data. The 1D model code, WAVEGEN, was developed by Robert Dean and is based on basic theories from Shore Protection Manual (1984) and Coastal Engineering Manual (2003). The code was provided directly by Dean. There are three test cases shown in Figures 18 to 22. In Cases 1 and 3, the waves are initialized at the offshore boundary with a JONSWAP spectra. In Case 1 we blew a 50 m/s wind to the north and started the

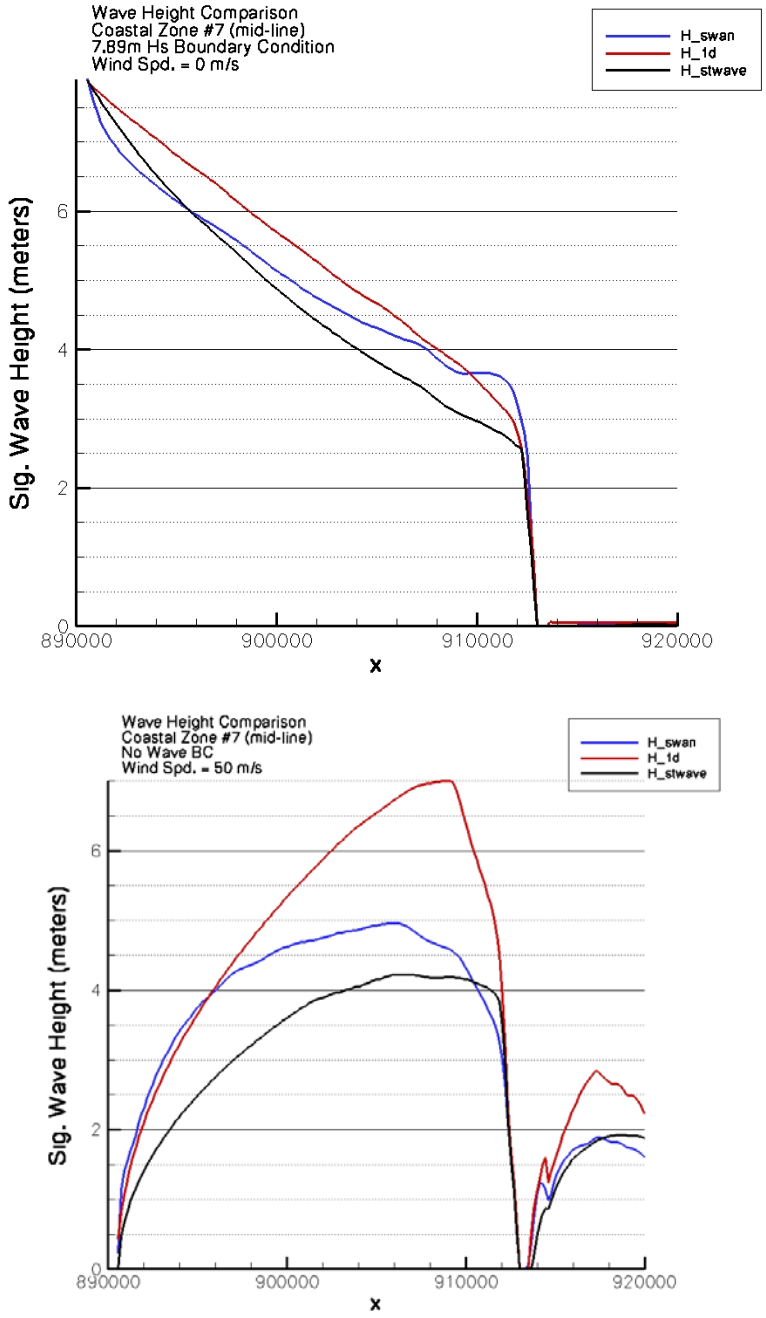

Figure 19. Comparison of SWAN, STWAVE and Dean's 1D model for no wind (Case 2) and zero offshore wave height as a boundary condition with a uniform wind of 50 m/s (Case 3) simulations. The top panel shows the wave heights for Case 2, and the bottom panel shows the wave heights for Case 3.

offshore significant wave height boundary condition at 7.89 m with a peak spectral wave period of 10 seconds. In Case 2 we used the same 7.89 m offshore significant wave height but did not blow a wind at all. And in Case 3, we blew the 50 m/s wind, but started the offshore wave height at 0 m. Each model has different wind wave input

parameterizations as well as different wave breaking models. These three tests are designed to illustrate the different responses from each of these features.

The bottom panel of Figure 18 shows the cross shore distribution of the wave height for Case 1. The wave heights predicted by STWAVE (black line) and SWAN (blue line) are quite similar. We note that the waves begin to break all across the shelf. Both models have white-capping terms that are significant in intermediate depth water, at reducing the wave height from approximately 8 to 4 meters. STWAVE is set to begin depth limited breaking when the ratio of Hs to the water depth is 0.6. SWAN has a more sophisticated, slope dependent depth limited breaking criteria. The waves decay from approximately 8 m to 4 meters before depth limited breaking plays a significant role. Then at around a water depth of 5 m, the waves in both models drop off rapidly in the Surfzone outside of the barrier islands. The surf zone in SWAN is wider than that in STWAVE, that is, the waves begin to break farther offshore. All three models predict wave height distributions in fairly close agreement inside the surf zone. The decay in wave heights from 8 meters to 4 meters is not caused by depth limited breaking, but rather by steepness limited breaking. As the wave spectrum becomes saturated, and the waves shoal in intermediate depth water, they shorten in wave length and cause the wave crests to steepen and break more regularly. This process transfers momentum to the water column, that leads to wave induced setup, but this happens in deeper water than would occur if depth limited breaking were operative. The wave radiation stresses are proportional to the wave height squared. Hence, a large portion of the wave momentum, is transferred to the water column in relatively deep water, allowing less momentum to amplify the setup in shallower water.

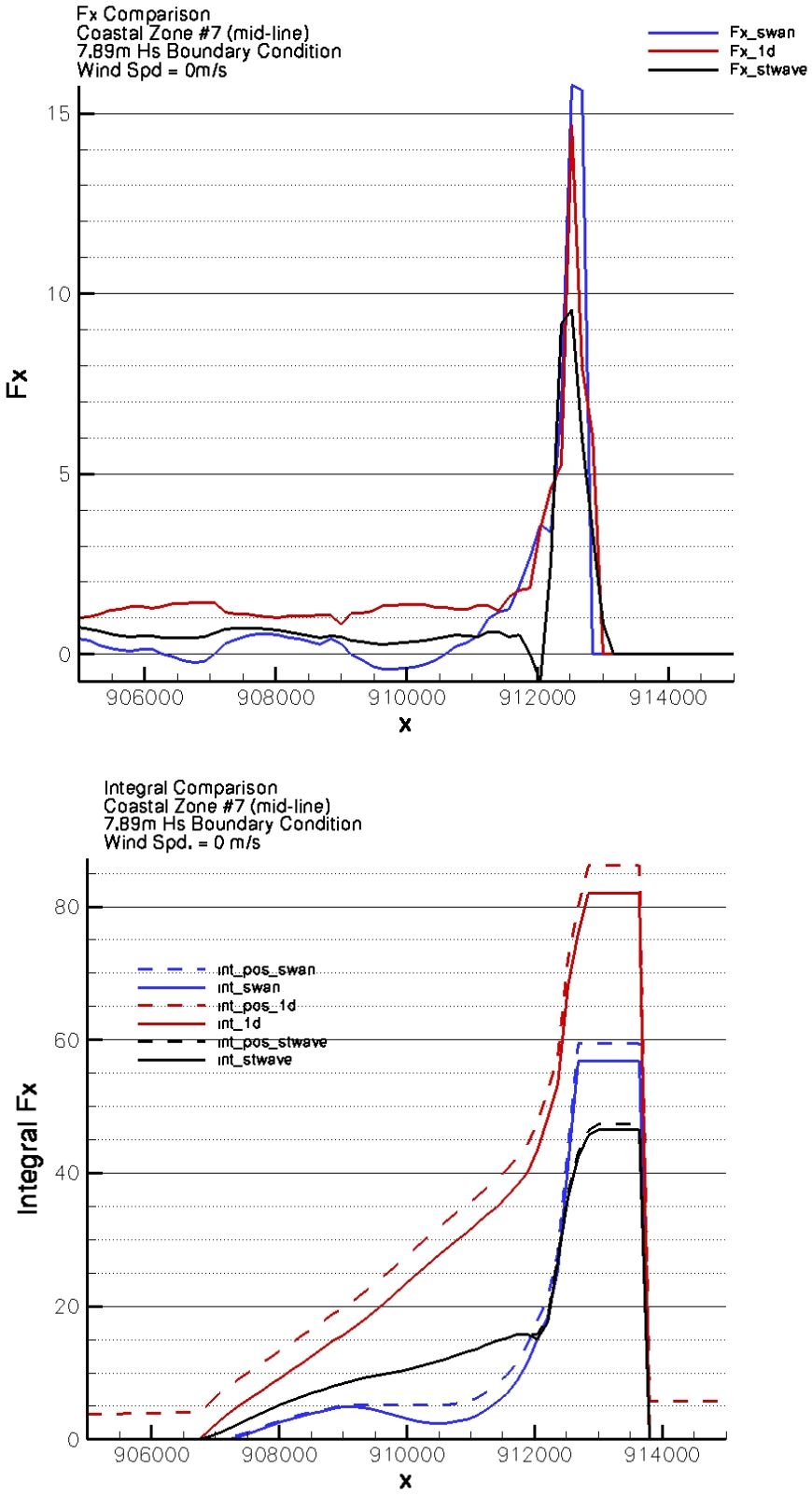

Figure 20. Cross shore force distribution (top panel) and total integral of the forces (bottom panel) for the three models applied in one dimension to Case 2.

Figure 19 shows the cross shore wave height distributions for Cases 2 and 3. It is evident that all three models handle the zone of depth limited breaking in similar fashions, but that they have very different wind-wave growth models. The 1D model has the largest wind-wave growth. STWAVE has the largest steepness limited breaking sink term in the wave action equation, and SWAN starts breaking waves in the surfzone sooner than the other models, because it includes a shelf slope dependent depth limited breaking criteria. Additional tests, not included here, showed that on steeper slopes, SWAN predicts later wave breaking in the surf zone than STWAVE. The present slope of 15 m change in depth over 8 km is a slope of approximately 1/500, or a relatively mild sloped shelf.

The cross shore distribution of the wave forces and of the cross-shore integral of the wave force are shown for Case 2 in Figure 20 and for Case 3 in Figure 21. The location of the start of the cross-shore integration was chosen as x = 907,000 m which is approximately the location of the change from wave growth to wave decay in Case 3 for all three models. This helped to minimize the bias in the results caused by beginning the integration at an arbitrary offshore location. A review of the wave force plots shows that the signals outside of the surfzone can be noisy. The noise was due in part to the combination of wave growth due to wind energy input and shoaling effect, and because the offshore boundary of the surfzone region differs between the cases. To assure that the noise was not interfering with the cross-shore integral, the integration of the wave force was done two ways, represented by the solid and dashed lines in Figures 20 and 21. The first methods was a direct integration of the wave force (solid line). The second consisted of integrating only the positive (shoreward) forces. The two methods appear to give slightly different results, but the differences are smaller than those between the individual models, and therefore do not affect the model-to-model comparisons.

In Figure 20, the integrals are shown for all three models for Case 2. At the starting point of the cross-shore integration, (907,000 m) the wave height in the 1-D model (4.4 m) is larger than the waves in SWAN (4.1 m) and in STWAVE (3.5 m) (top panel of Figure 19). These differences are because the models have different formulations for bottom friction and steepness limited breaking or white capping that cause wave decay outside the region of depth limited breaking (which begins near x = 911,000 m). SWAN predicts larger wave forces in the surf zone than STWAVE, because there is less loss of wave momentum by steepness limited breaking farther off shore. The SWAN surf zone starts farther off shore. The total integrals for the SWAN and STWAVE models give similar values. The Dean model gives a larger total integral. As mentioned, the offshore wave heights differ between the models at the point where the cross-shore integration is started, and therefore the total integral of the force will differ similarly (by the square of the offshore wave height) as observed, because the total wave force integral necessarily scales as the offshore wave height. Note also, that if the offshore location of the integration were chosen to be at x = 890,000 m, then for Case 2 all the models would give the exact same answer. This result will not occur in Case 1 or Case 3, because they have different maximum wave heights due to differing wind-wave growth models. This comparison of the wave force and its integral shows the consistency between the models,

in that a wide surf zone (such as produced in SWAN) gives nearly the same total force as a narrow surf zone (such as produced in STWAVE) when the two models start with the same wave heights outside their respective surf zones.

Figure 21 shows that the Dean model yields much higher wave set up because the wind wave growth model is so much stronger than for the spectral wave models. The total integral of wave momentum transferred to the water column between SWAN and STWAVE are nearly identical (bottom panel of Figure 21). Again, the surf zone from SWAN is wider than for STWAVE. For the case of Figure 21, the peak values of the force from STWAVE in the surf zone are about twice as large as the peak values of the force from SWAN. This is again because of the variation in the width of the surf zone.

Finally, Figure 22 shows a comparison of the setup for the region outside the barrier islands for Cases 1 through 3. The direct comparison is only valid offshore of the barrier islands and the comparison in the Mississippi Sound should be ignored. Landward of the barrier islands the direct comparison is lost, because the different models integrate the setup across the barrier island differently, either assuming a flooded island scenario (SWAN uses a continuous ocean assumption), or assuming a non-flooded island scenario (STWAVE uses a separate ocean basin assumption). The setup is related to the wave forces through the steady state relationship:

$$\frac{\partial \bar{\eta}}{\partial x} = -\frac{1}{\rho g\left(h+\bar{\eta}\right)}\frac{dS_{xx}}{dx}$$

Where η is the mean water surface (the setup), h is the water depth, and S_{xx} is the radiation stress. The key difference between the integral of the forces and the setup is that the setup has the water depth, h, in the denominator, making the setup very sensitive to the width of the Surfzone and the depth at which the waves break. For Case 1, STWAVE predicts larger total setup than SWAN. For Case 2, SWAN and STWAVE predict the same total setup within a few percent. For Case 3, SWAN predicts somewhat larger total setup outside the barrier island than STWAVE. In summary, the models are somewhat different, either one can give large values of setup than the other depending on details of the wind and offshore wave amplitudes and the shelf bathymetry. Both models give very similar results, usually within about ten or twenty percent of each other. The 1-D model has many similar properties, but is often predicts setup about twice as large as the 2-D spectral models, when run in 1-D mode. The primary differences are the wind-wave growth model and the steepness limited breaking sub-models. We note, from our experimentation, that if the breaker height index in STWAVE is set to 0.42 instead of the default value of 0.6 that the results for wave height and setup between SWAN and STWAVE for this particular bathymetry become very similar. One of the authors of STWAVE (D. Resio, private communication) has indicated that he feels that this adjustment would be justifiable on a mild sloping shelf.

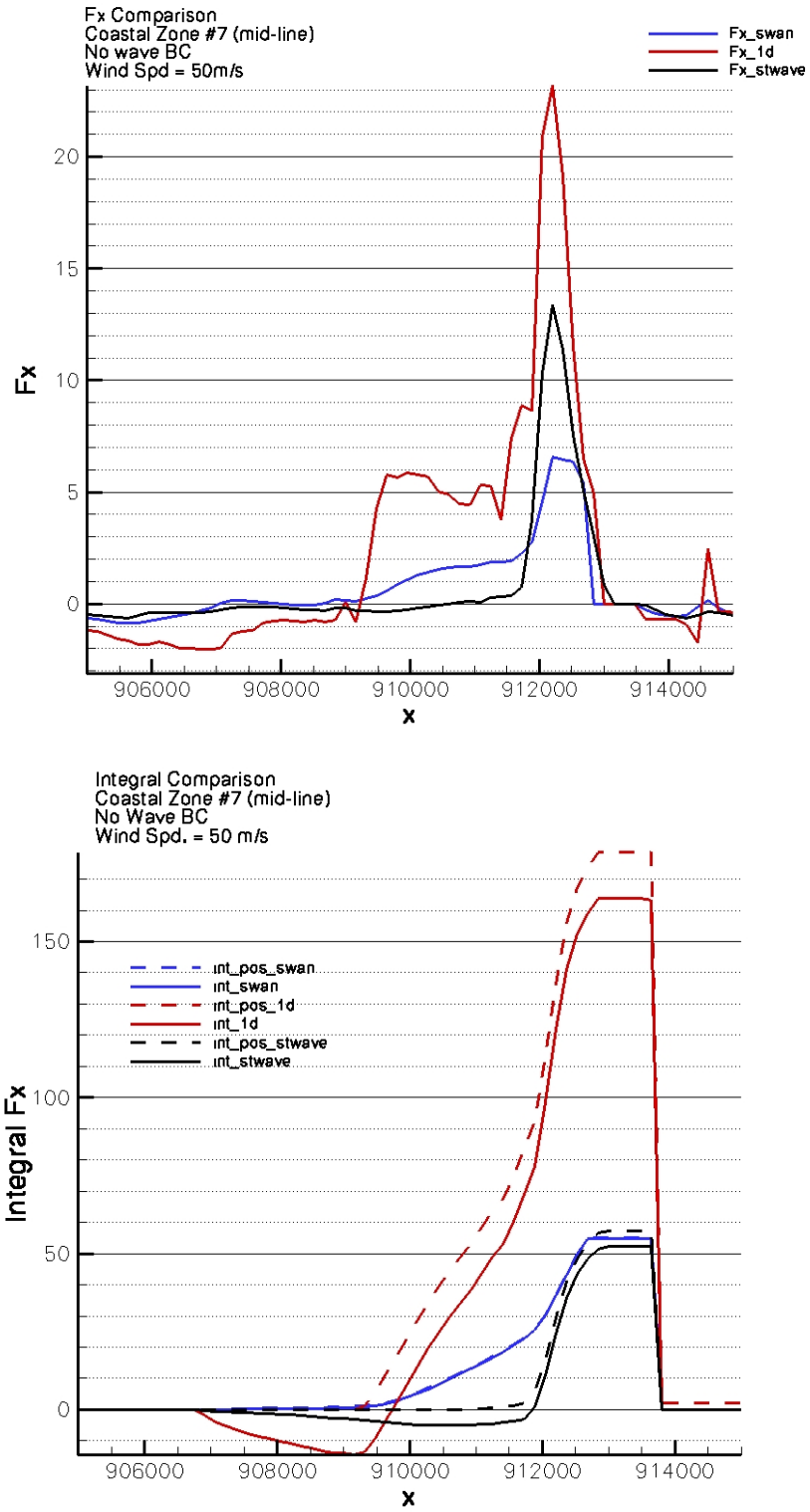

Figure 21. Cross shore force distribution (top panel) and total force integrals (bottom panel) for the 3 models for Case 3.

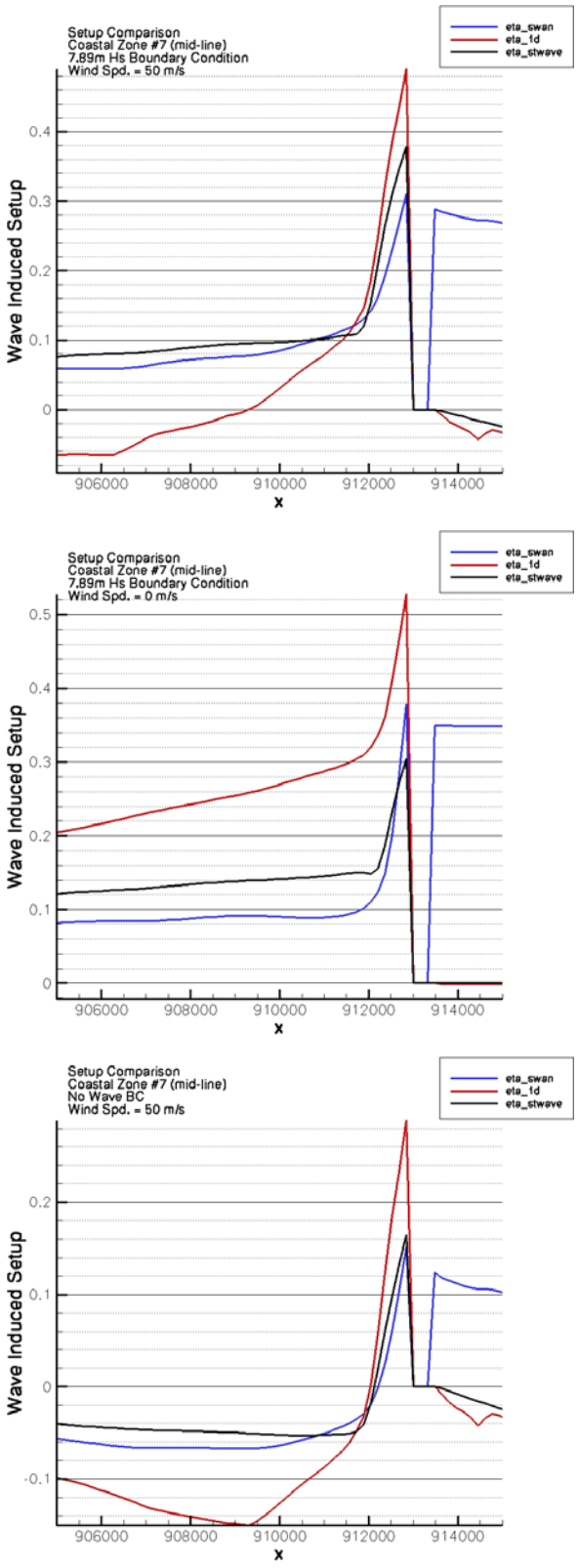

Figure 22. Results for setup (in meters) of the three models for all 3 cases (Case 1 top panel, Case 2, center panel; Case 3, bottom panel).

5.4 Example Wave Setup Results in the Mississippi Study

The contribution to the total storm surge from the wave setup has been examined in a number of ways. The flow response to a hurricane is a non-linear process and linear superposition of solutions is not an accurate method of determining the separate contributions of wind and waves. We present results of two (of many possible) methods for quantifying the total wave setup contribution to the total storm surge. Results are shown in Figures 23 to 28. Results range from approximately 0.15 to 0.85 meters depending on how conservative of a definition is used. There are three basic definitions that are relevant. ADCIRC can be forced with three different stresses: (1) the wind and pressure fields; (2) the wave stress fields; and (3) the combination of wind, pressure and wave stresses together. The first definition of the wave setup contribution to the total storm surge is to run (1) and (3) and determine the difference between the Maximum Water Levels during the simulation between these simulations. The second definition of the wave setup is to determine the maximum difference between the time dependent water levels between these two simulations at any time. The difference between these first two definitions is that the maximum contribution from the wave forces does not necessarily occur at the same time as the maximum total flood occurs. The maximum total flood levels in the coastal domain do not occur at the same time everywhere. The MEOW (maximum envelope of water) is not a snapshot of the water levels everywhere at the instant when the maximum local water level occurs at some point. But instead they represent the maximum water achieved at any time by the total flood at every individual point. Following that same logic, the maximum envelope of the contribution of the wave setup to the total flood, using the second definition, could show the maximum difference in time dependent flood levels. We have found through experience that the second definition often gives values that are twice as large as the first definition. This is consistent with the understanding that the hurricane waves usually reach the shore before the hurricane winds makes landfall. There are conditions when only the maximum flood levels are significant for design guidance, and there are other applications, such as time dependent scour around bridge piers, when knowing the entire hydrograph (the time dependent water levels during a storm) is important to safe design and coastal construction. Similarly, the maximum waves do not necessarily occur when the maximum flood is present at a given location, because they may depend on local wind conditions. While it is likely that FEMA is usually most concerned with the maximum water levels at a location, there are other instances when determining the maximum waves at a location would be most important for construction design guidance.

The third definition for wave setup is to run the ADCIRC simulation driven by just the wave forces and to find the maximum envelope of water. We present results below for definitions one and three. There are several physical reasons why these give different results and so they should be interpreted with care. We note that the contribution of waves to the total surge is strongly dependent on the shelf slope. On a steep slope the waves make a much larger relative contribution. Mississippi has a very broad shallow shelf, a condition that maximizes the contribution to the total surge from the wind stress, and minimizes the contribution to the total surge from the wave stresses. Hence, the results for Mississippi are not expected to be typical of results for other

Coastal States with different Continental shelves. For example, as shown below, the wave setup for the same storm on the Mississippi Delta is approximately three to four times as large as the wave setup modeled behind the Mississippi Barrier Islands.

Figure 23 shows the spatial distribution of the wave setup from simulations of Hurricane Katrina on the MS11 ADCIRC grid, using definition (1) above, along the eastern Mississippi coastal zone. In much of this region the setup contributes approximately 10 to 15 cm to the maximum water levels. Figure 26 below shows that this region is the area with the lowest wave setup in the Mississippi – Louisiana coastal domain.

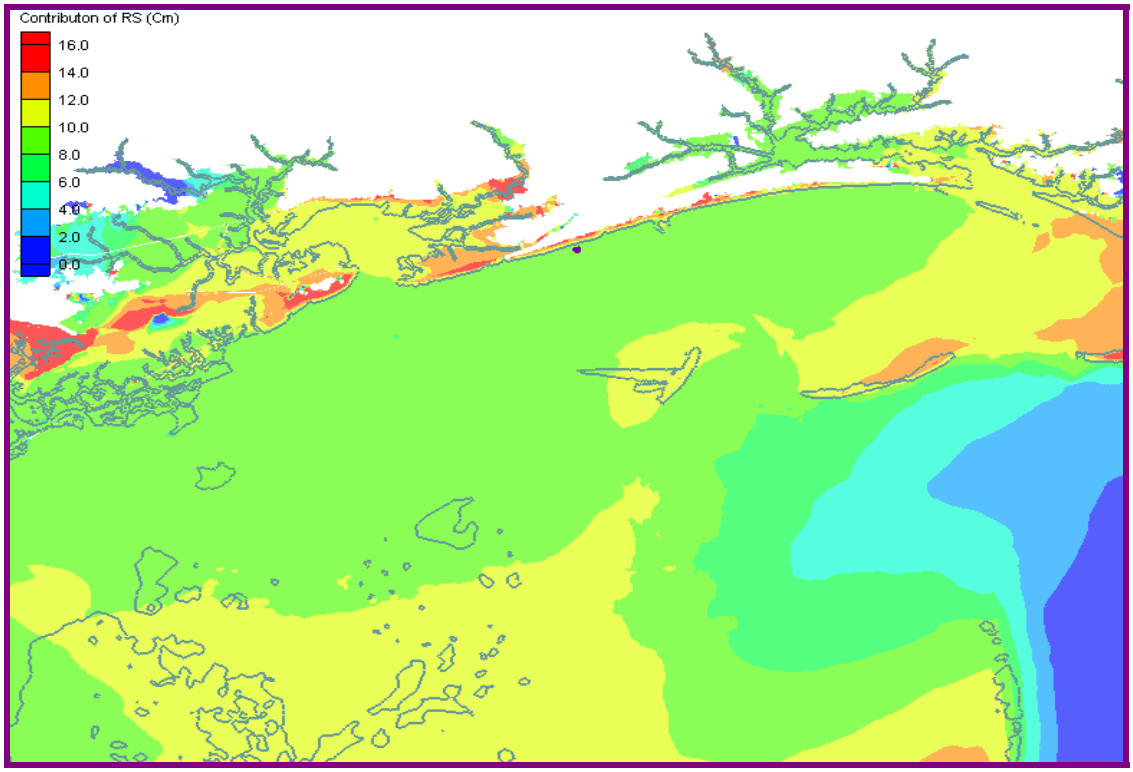

Figure 23. Wave Setup for Hurricane Katrina in Mississippi Coastal Area determined by the difference in the maximum flood levels when forced by wind with and without waves.

Figures 24 and 25 show the water surface elevations at the times of maximum flood levels (between 6 and 8 meters) along a transect from the barrier island to the shoreline in the eastern section of Figure 23. Along this transect the setup at maximum flood levels is between 9 and 15 cm.

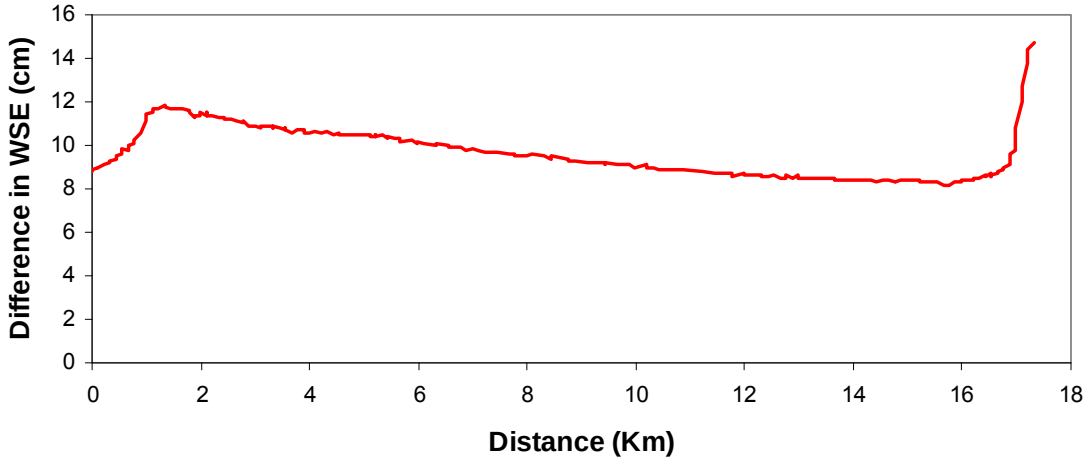

Figure 24. Difference in Water Surface Elevations for Hurricane Katrina along a transect from the barrier islands (located at x=0) to the shoreline determined by the difference in the maximum flood levels when forced by wind with and without waves.

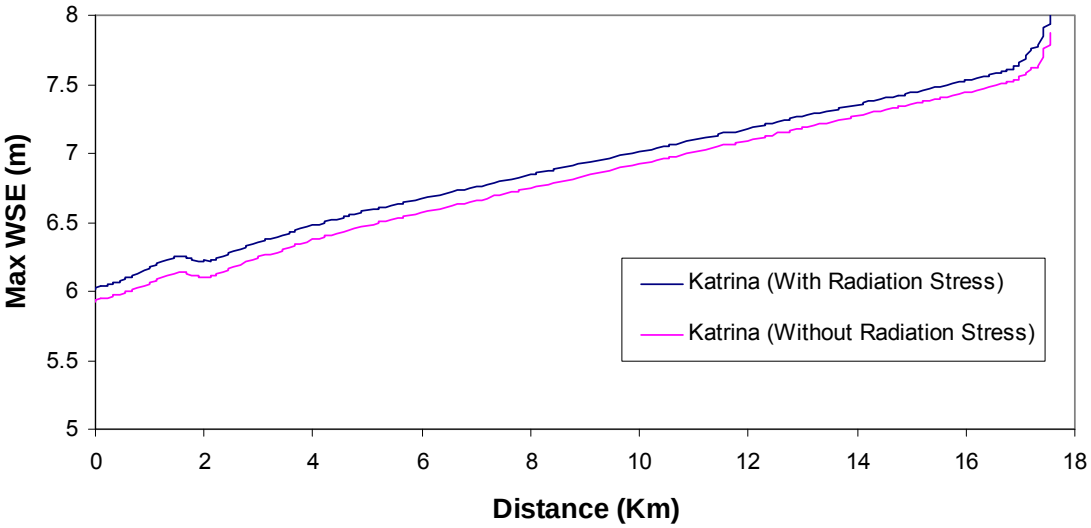

Figure 25. Water Surface Elevations for Hurricane Katrina along a transect from the barrier islands to the shore line during conditions of maximum flood levels when forced by wind with and without wave forces added.

Figures 26 to 28 show the Setup determined using definition (3) above. Here the ADCIRC model is forced only with the wave forces from Hurricane Katrina and the envelope of maximum water levels is extracted. Values of wave setup along the Mississippi coast range from 10 to 35 centimeters. Values of wave setup along the Mississippi Delta are up to 87 centimeters.

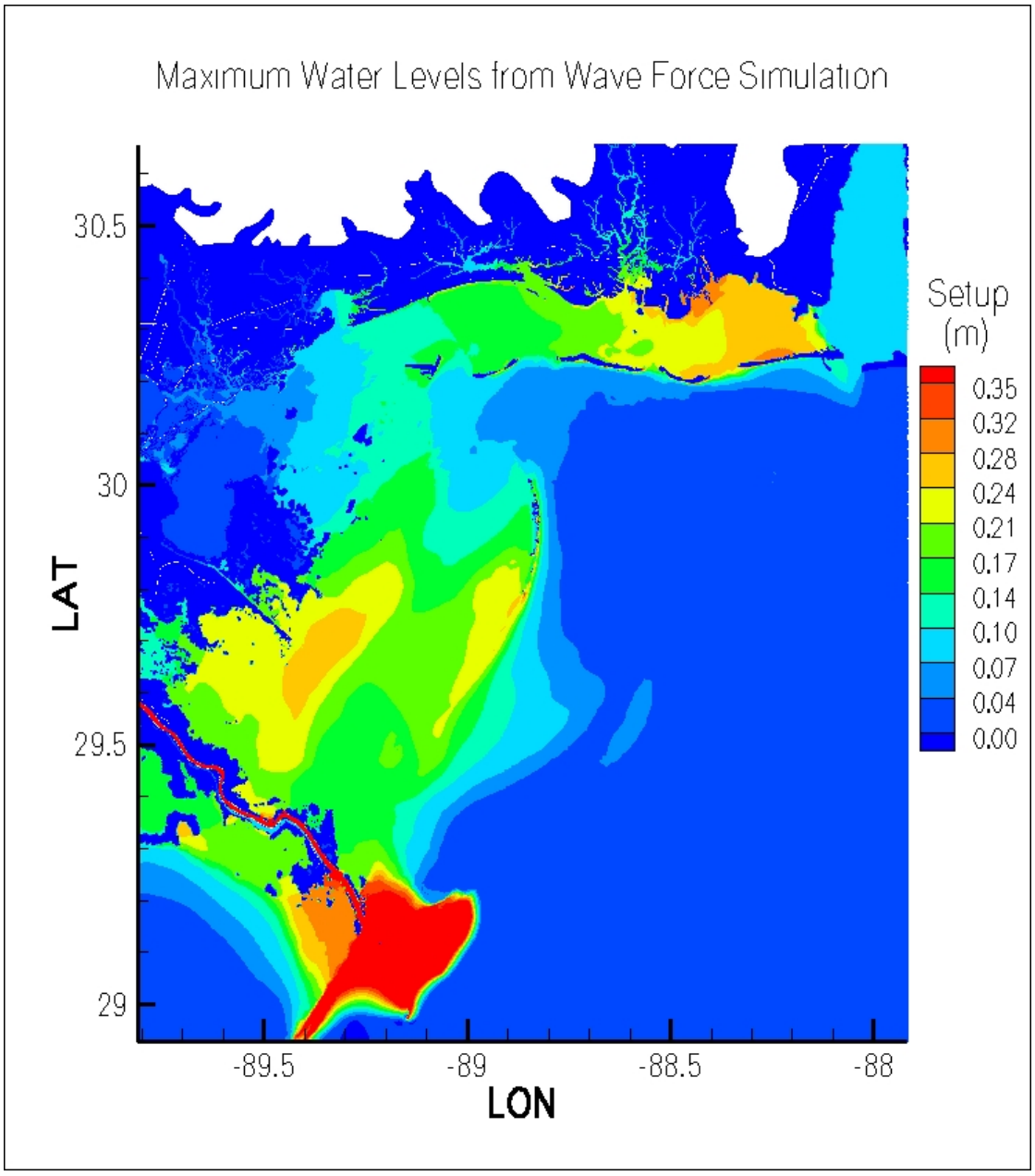

Figure 26. Wave Setup for Hurricane Katrina in Mississippi Coastal Area determined by the difference in the maximum water levels when forced by waves only.

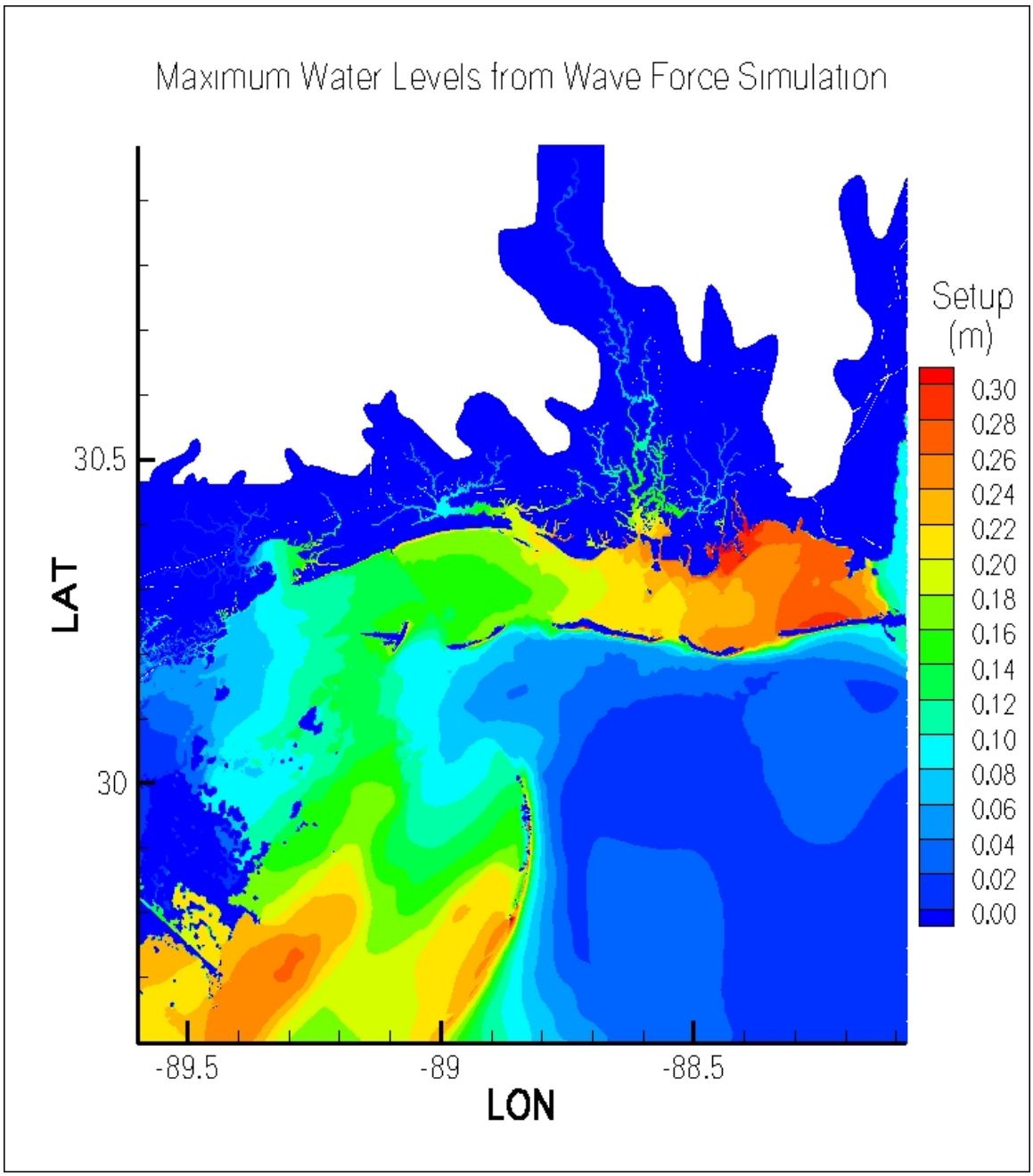

Figure 27. Wave Setup for Hurricane Katrina in Mississippi Coastal Area determined by the difference in the maximum water levels when forced by waves only.

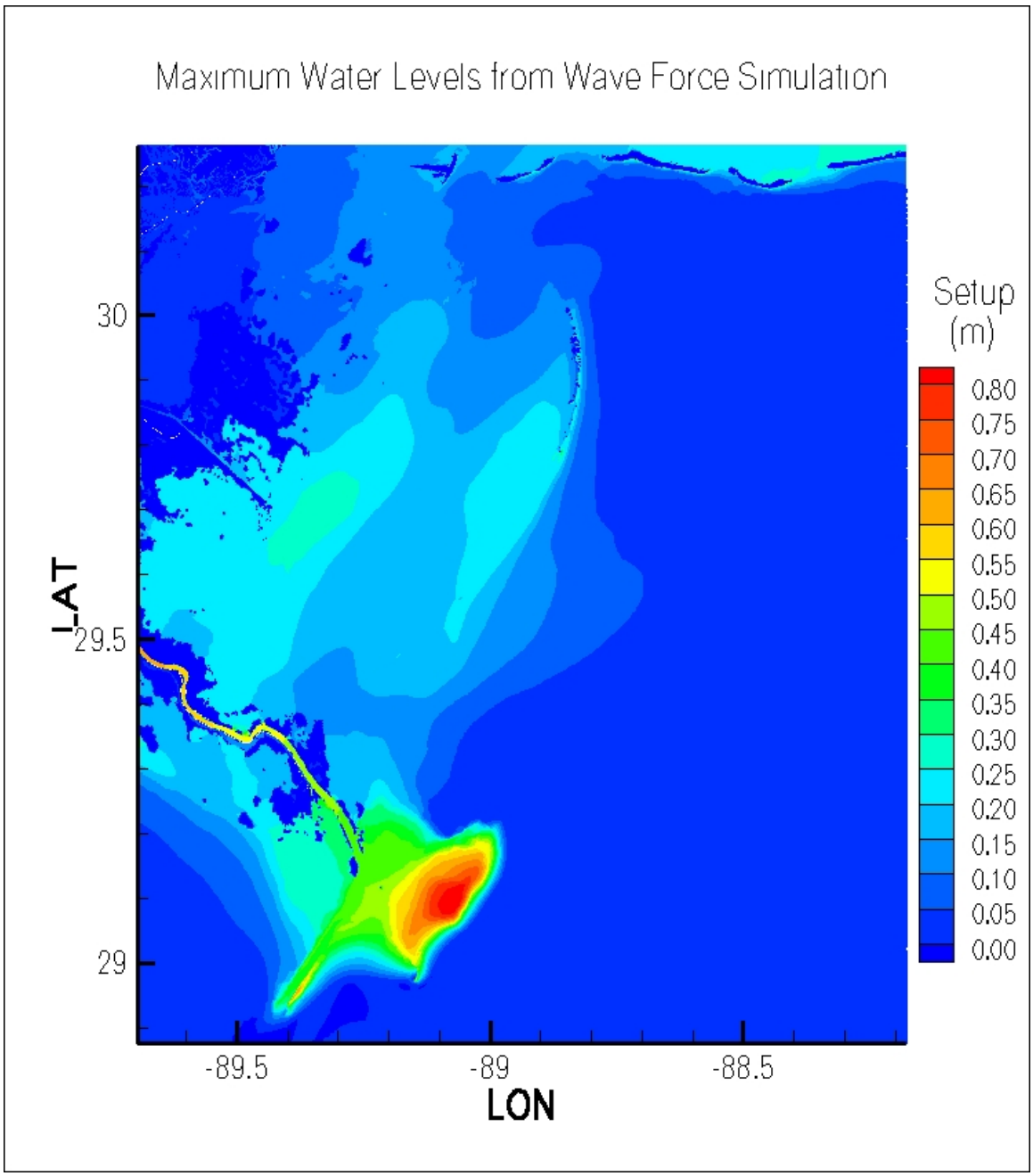

Figure 28. Wave Setup for Hurricane Katrina in Mississippi Coastal Area determined by the difference in the maximum flood levels when forced by waves only.

There are a number of reasons why the different definitions yield different results. These include different degrees of flood inundation across the low flat terrain. As the wind and wave pushes water inland, the extent of the flood changes depending on the total stresses. A second contributing factor is that when the flood levels are high locally they tend to spread alongshore as well as inland. The larger the local floods, the greater the rate at which the water flows along the shore. Thus, wave setup on top of a storm surge surface, experiences different currents and pressure gradients compared to the wave setup that is produced by wave forces only.

6.0 Production Runs and Model Output QA / QC Procedures

Wave fields were calculated using Basic Wave Setup Modeling System for the 228 storms used in the coastal flood hazard surge modeling. The radiations stress outputs were compiled into fort.23 input files and provided for use in the ADCIRC surge modeling analysis.

Each simulation was verified during the production run process. This was accomplished in two ways. We wrote a code that looked for any anomalously large values of wave height, period, or force beyond anticipated thresholds. For example, wave heights over 30 meters would be unlikely to be physically plausible and signal model problems. We also made plots of the maximum wave heights and forces in the region and coastal domains. A set of these four plots is include here in Figure 29 – 31 for Simulation # JOS6013E. Figure 29 shows the maximum force, written to the Finite Element grid for the ADCIRC fort.23 file over the duration of the storm. The units of force are m^2/s^2, the stress normalized by the density of water. In order to limit the file sizes to a much more realistic file size, ADCIRC allows that only non-zero, or finite amplitude, forces be written. This decreases the file size by two orders of magnitude, because many of the finite element nodes are dry or outside of the region of interest.

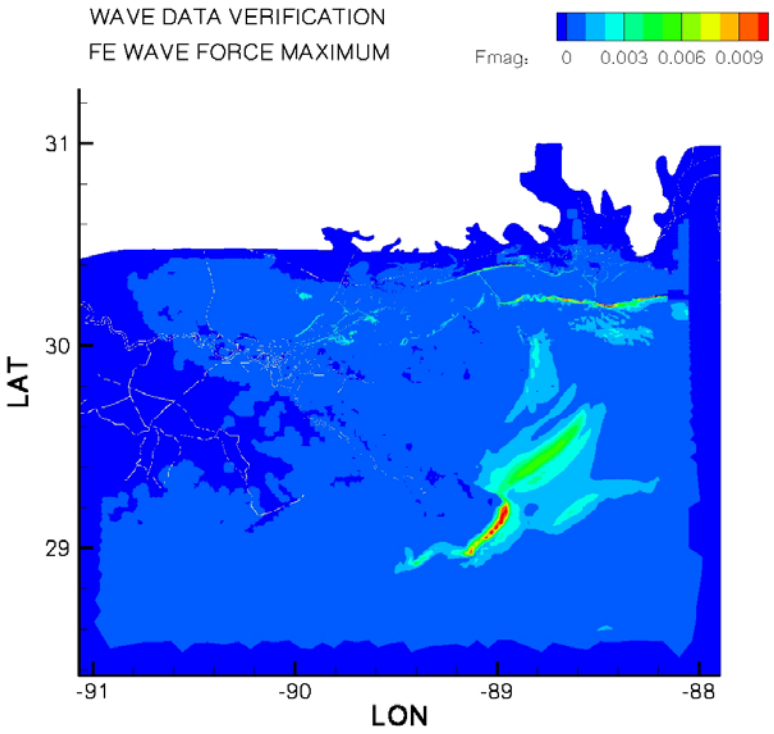

Figure 29. QA / QC plot of Maximum forces in the Region domain for JOS6013E.

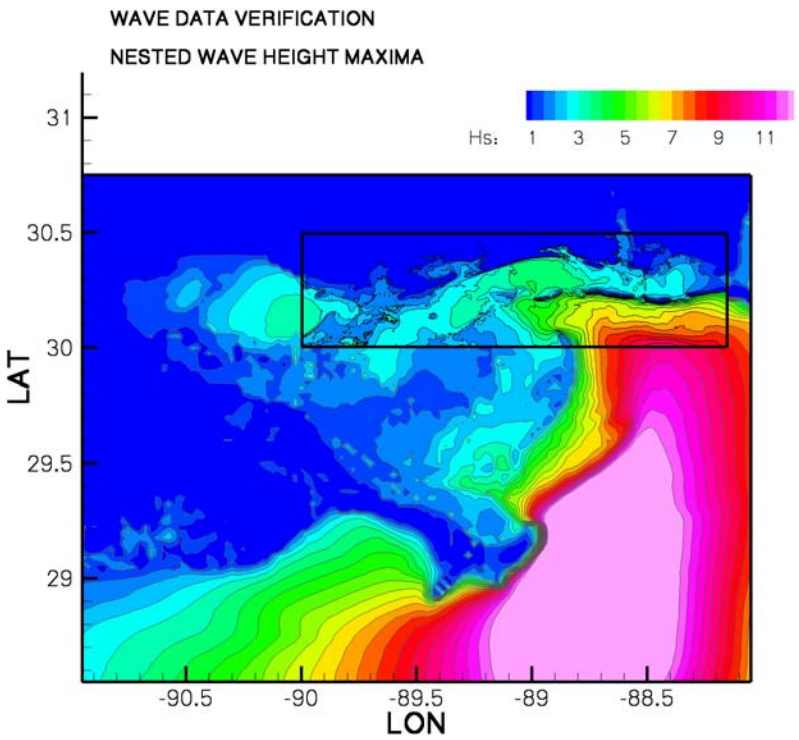

Figure 30. QA / QC plot of Maximum wave heights in the Region domain for JOS6013 with the nested Coastal Domain shown in the black rectangle.

Figure 30 shows the QA/QC plot of the regional maximum significant wave heights (in meters) achieved over the duration of the storm (JOS6013E) and shows the high resolution nested domain. The plots were generated automatically for each simulation as part of the master script, using Tecplot and Fortran. Each was examined by a trained team member before the wave forcing files were passed on to the next step of the modeling process.

Figure 31 shows the Maximum Significant Wave heights (top panel) for Production Run (JOS6013E) and the magnitude and direction of the maximum wave forces transferred to the storm surge model ADCIRC in the coastal domains. We note that the waves and wave forces are time dependent, with new fields written to the ADCIRC input file every 30 minutes, but that by examining the maximum values that occur during the course of the simulation we are ensured that the fields remained appropriately bounded for the entire duration of the storm. Movies of some of the wave fields were made to ensure that the wave fields evolved properly.

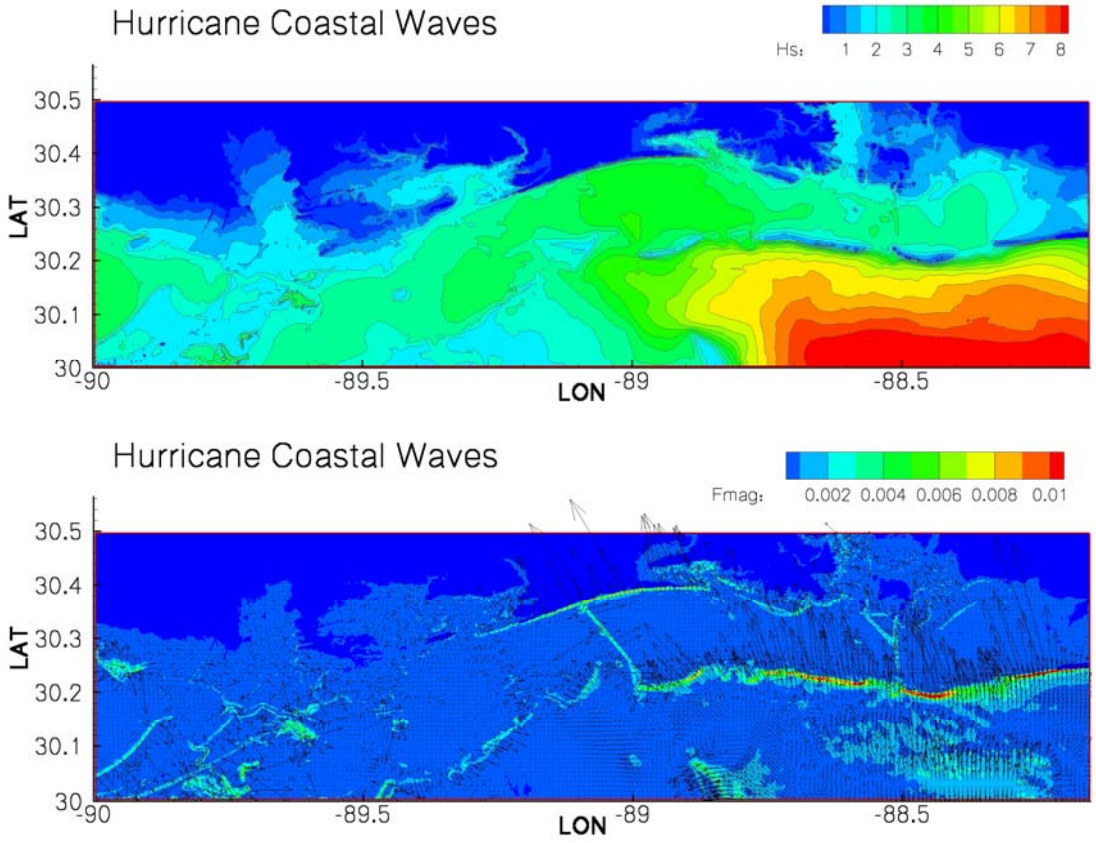

Figure 31. QA / QC plot of Maximum wave heights in the coastal domain (top panel) and the magnitude and direction of the maximum wave forces in units of m^2/s^2 for JOS6013E.

7.0 Calculation of 100 and 500 year Wave Heights for WHAFIS Transect Analysis

The wave fields were also used to provide improved estimates of offshore wave conditions for the Overland Wave model WHAFIS. The outputs from the production runs provided wave heights and periods as well as the radiation stress gradients, so it was therefore straightforward to determine the wave heights associated with the 100 year and 500 year flood levels. This was done in a somewhat sophisticated manner, because of the averaging techniques that went into determining final 100 and 500-year flood levels. For each of the production runs, we made files of the maximum water elevations and of the maximum waves achieved at each grid point in the coastal domains. We also made a file of the average wave periods associated with the time when the maximum waves occurred. We then rank ordered the water levels at each of our 333,000 coastal wave grid points, in a similar manner to what was done to determine the URS estimate of the 100 year flood level. We then took the wave heights, as they were ordered by their associated water levels, and did a linear regression of the wave heights to produce a smooth function describing the wave height associated with each return interval. Using the probability of

each storm, it was then straightforward to determine the 100 and 500 year water elevations and their associated wave heights. This gave us a least squares best fit linear relationship between the flood levels from each storm and the wave heights for each storm. Then we used this relationship, and the final, 100-year flood level to determine the most likely value of the 100-year wave heights at the 161 WHAFIS wave transect start points along the Mississippi Coast. Plots of the relationships between the wave heights and the water levels were made for each point.

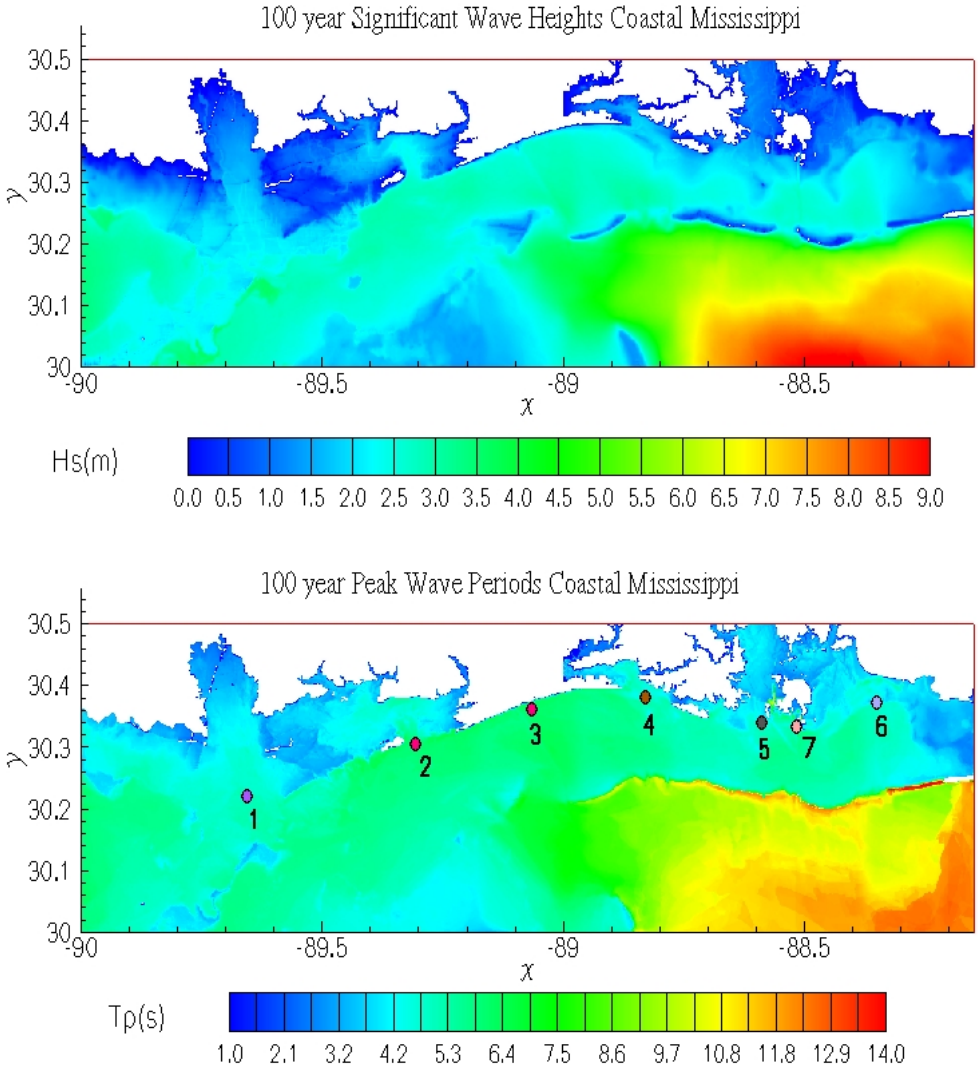

Figure 32. Coastal Mississippi region, plots of 100 year wave heights and mean periods, determined by rank ordering of storms.

Figure 32 shows the 100 year wave heights and periods determined in the coastal Mississippi region using the rank ordering approach for the 152 Category 3 to 5 storms. Peak wave periods, Tp, in excess of 12 seconds are common outside the barrier islands, but wave periods of 5 to 7 seconds are more common inside of Mississippi Sound. Figure 33 shows a more detailed view of the 100 year wave heights and periods in the

Western Mississippi coastal region. These values were used as estimates for the Whafis Transect start points.

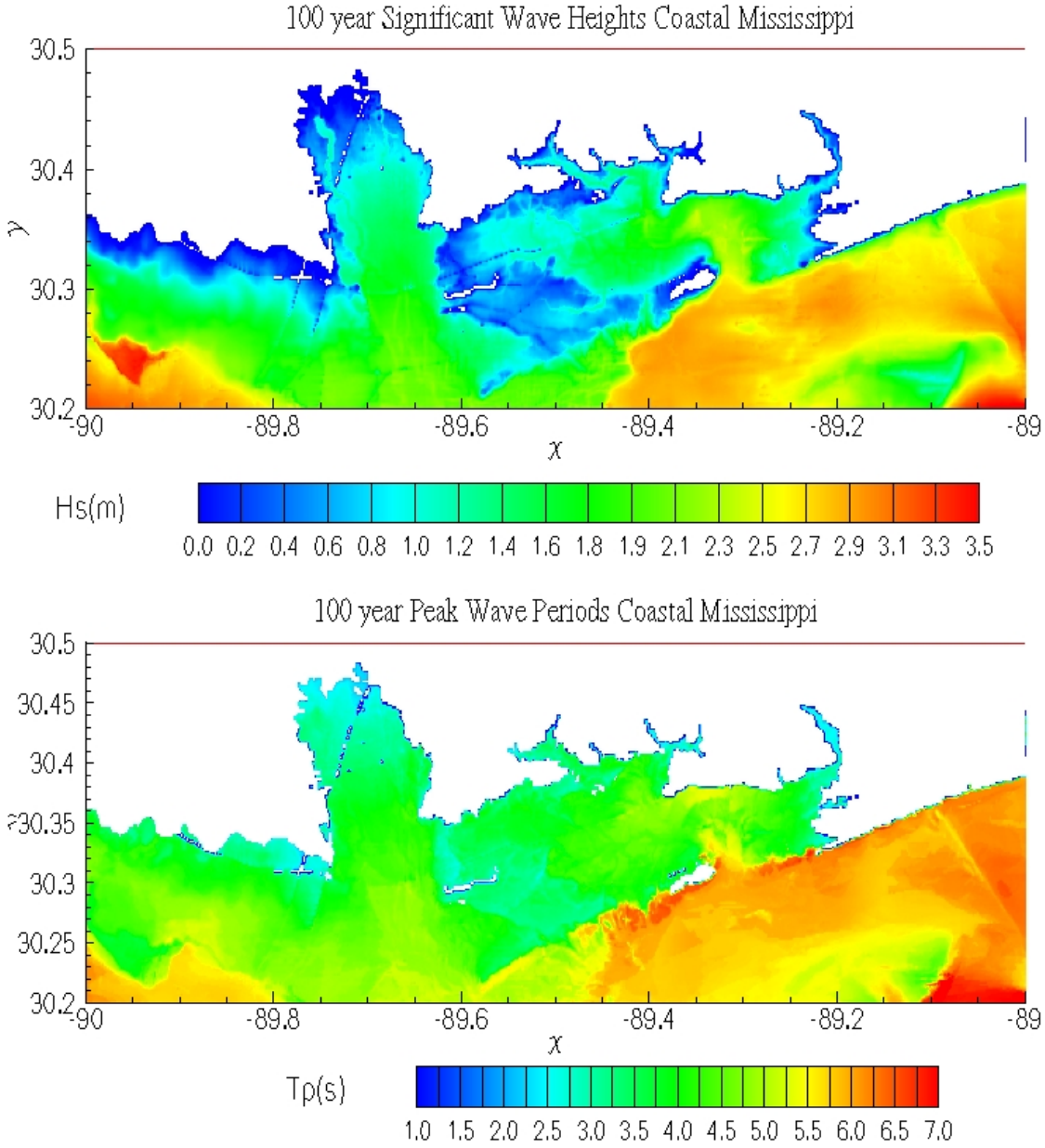

Figure 33. Close up of coastal region in western Mississippi for 100 year wave heights and periods, determined by rank ordering of storms.

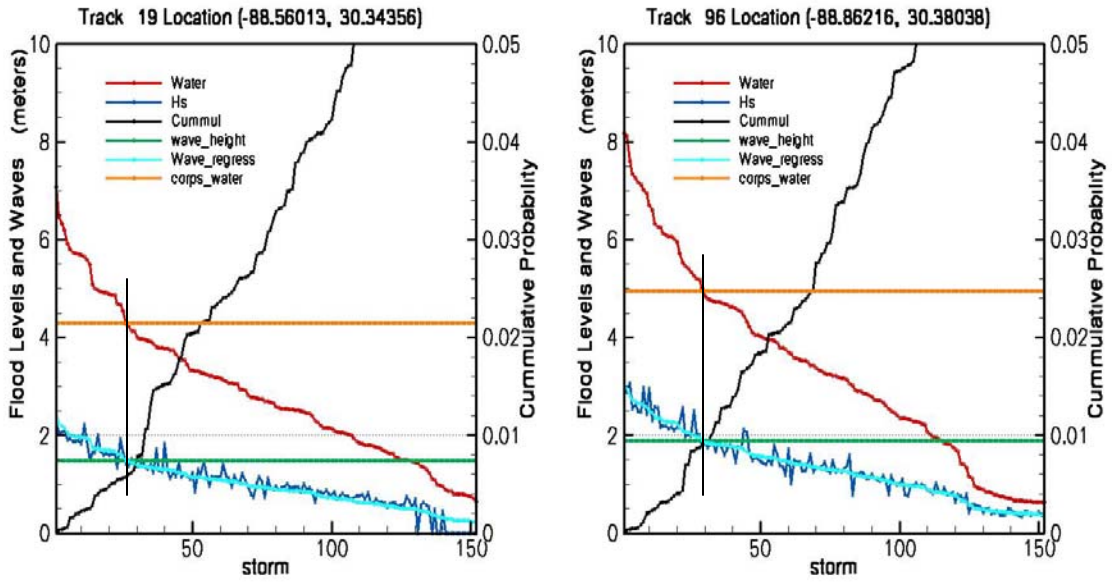

Figure 34. Rank ordered water levels (red line) for the 152 coastal storms at two of the Whafis transect start points. Also shown are the wave heights for those storms (dark blue line) and the linear regression fit (light blue line) that was used to estimate the 100-year wave height at each point. The orange line is the 100-year flood level, which was used to determine the final 100 year wave height (shown in the green line) for this point. The vertical line joins the points where the 100 year flood level and 100 year wave heights align.

Figure 34 graphically illustrates some of the intermediate steps of determining the 100 year wave heights. The water levels (red line) are rank ordered and the wave heights are ordered according to the associated storm water level. This yields the jagged dark blue line. The wave heights ordered in this manner correlate well, although not perfectly, with the surge heights, which is expected because the correlations are done in shallow water where depth limited breaking is a dominant. A linear fit is made between the wave heights and rank ordered water levels (light blue line).

The cumulative probability of each storm 1 through 152 (for the Cat 3-5 storms) is plotted in the black line. The 100-year water level is indicated at the point where the black line crossed the 0.01 threshold on the right y axis (intersection of the dashed horizontal line and black line). The vertical extension of this intersection to the blue line identifies the associated 100 year wave height. Note that the URS approach for identifying the 100 year water level incorporated uncertainty information that is not represented in the graphical example. Their methods yielded slightly different red and black lines. Therefore, to include the effects of uncertainty, and assure consistency with the URS approach, the URS 100 year water levels were used directly in the water level and wave height correlation (red and light blue lines) to obtain the 100 year wave height.

To get the wave period associated with the 100 year wave heights another estimate is used. Here, a second linear regression is done, between the wave periods and

the wave heights and then that formula is used to determine the final 100 year wave period based on the 100 year flood level and wave heights.

The 500 year wave heights are larger than the 100 year wave heights. The same procedures were used to determine the 500 year wave heights and periods as were used for the 100 year levels. Figure 35 shows a plot of the 500 year wave heights in Bay St. Louis. A table of the 100 and 500 year wave heights at the offshore locations used for Whafis are given in Appendix A below.

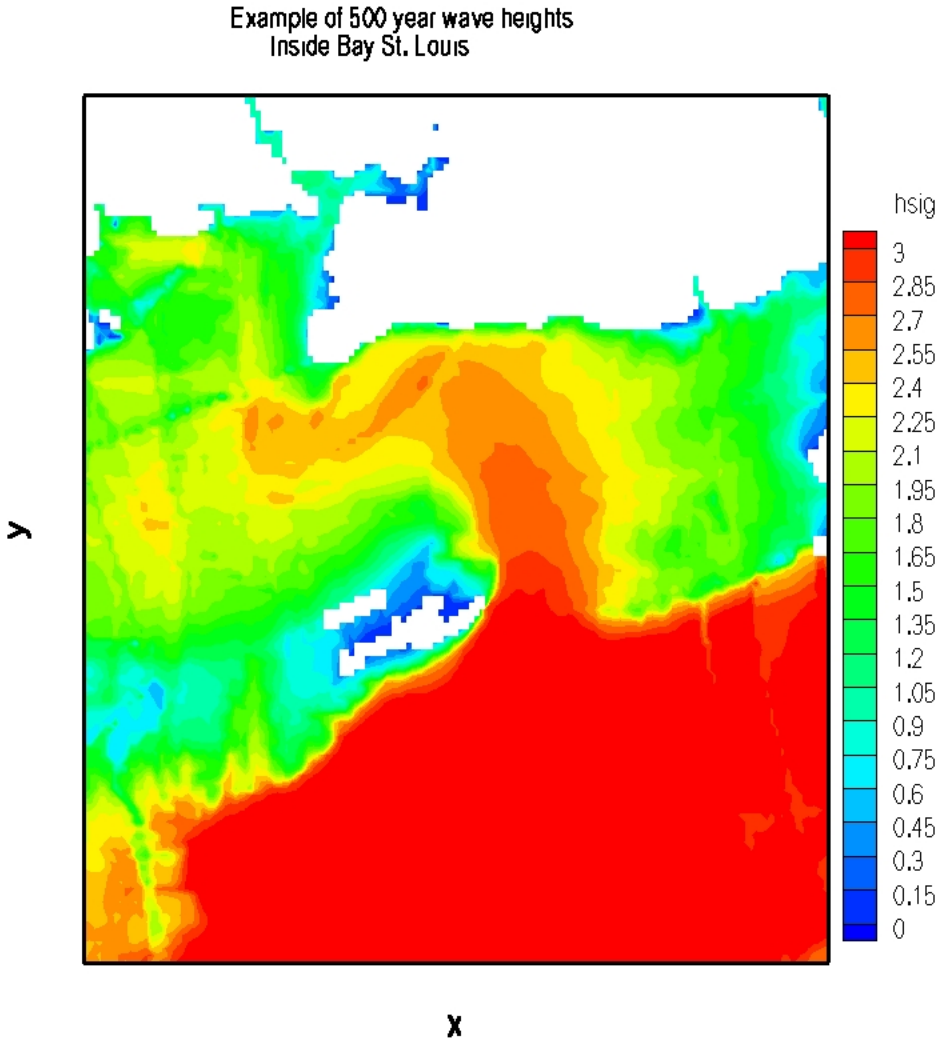

Figure 35. 100 year significant wave heights calculated by rank ordering of the flood levels from large storms. Shown here in the Bay St. Louis region.

Wave spectra were examined to see if the choice of the peak wave period was appropriate in the coastal region at 161 locations for several different simulations. Wave run-up is sensitive to the wave period, and determining the shape of the spectra could

influence the choice of runup modeling. The issue examined was whether or not double peaked spectra were common in the coastal zone. Approximately 20 spectra were examined over the duration of several strong storms. Figure 36 shows the locations and numbering of some of the points examined. The spectra at transect location 30 and 127 are shown in Figure 37 for storms number JOS6001F and JOS6014B respectively. If the spectra were strongly double peaked, it might have been important to utilize wave periods associated with the longer period (around 10 second period) waves instead of the short period waves (around 5 second period) that dominated the results.

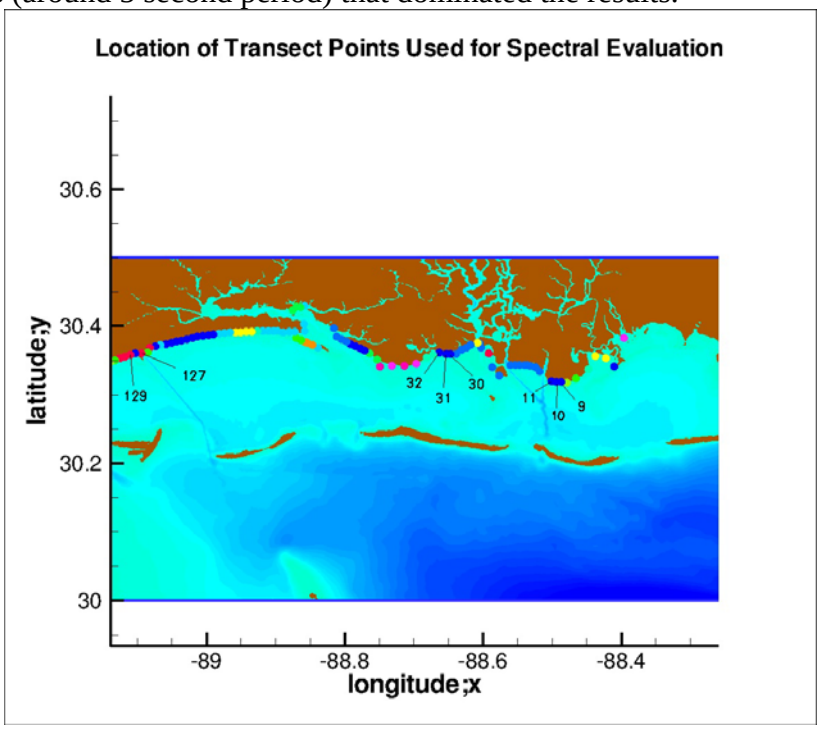

Figure 36. Location plot for wave energy spectra plots.

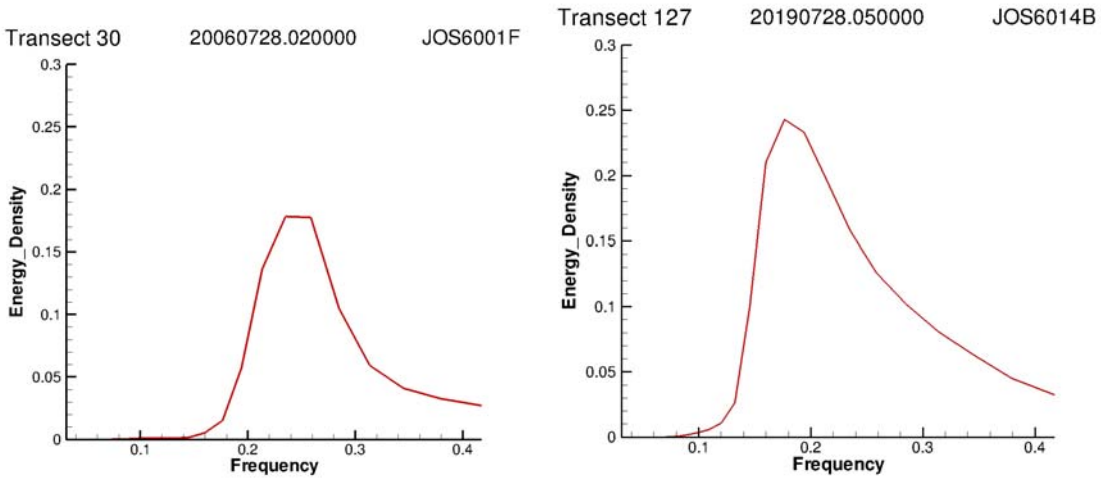

Figure 37. Wave energy spectra for Simulations JOS6001F and JOS6014B at transect locations 30 and 127. These spectra were used to verify and validate the wave periods used for the Whafis Transect start point and for determining relationships between different wave periods for wave runup calculations.

We found only three double peaked spectra anywhere along the Mississippi Coast. Figure 38 shows the double peaked spectra that occurred at point 2 in Eastern Mississippi. For this and the 2 other double-peaked spectra, the secondary peak at lower frequency contained much less energy than the peak near 4 to 5 seconds, approximately 10% of the energy in the higher frequency band of the spectra. The conclusion was that it was appropriate to use the higher frequency peak of the wave spectra in every case.

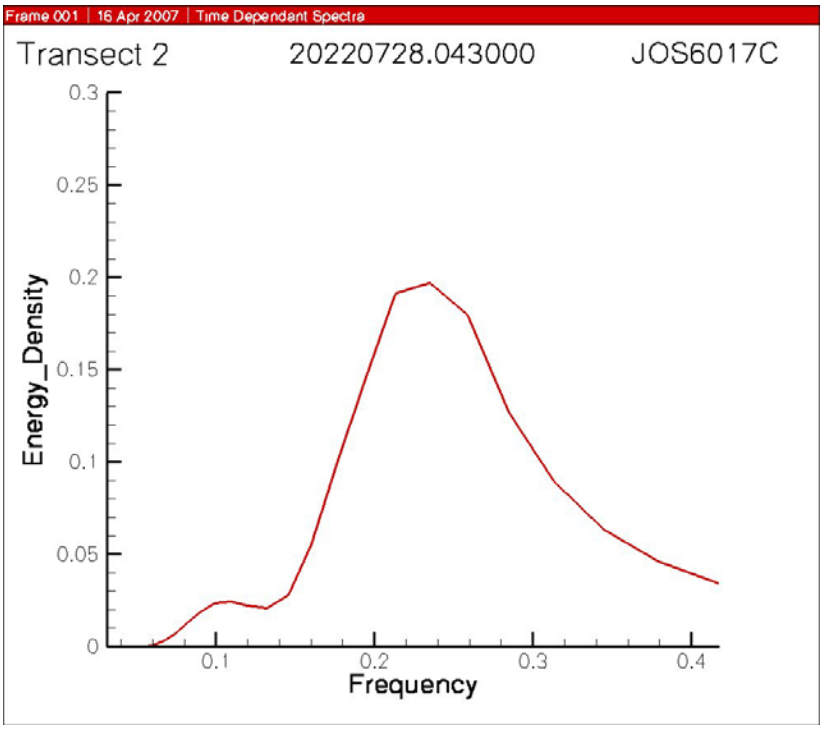

Figure 38. Wave energy spectra for Simulations JOS6017C at transect location 2. This spectra showed a double peak with energy at frequencies of 0.1 Hz (10 second period waves) and 0.24 Hz (4 second period waves) used for the Whafis Transect start point and for determining relationships between different wave periods for wave runup calculations.

Summary and Conclusions

The two-dimensional spectral wave model SWAN (Simulating Waves Nearshore) was used to calculate wave fields and wave radiation stress gradients in the coastal ocean for the URS FEMA Mississippi Coastal Flood Mapping Study. It was coupled to the storm surge model in several ways. The validity of the SWAN model was demonstrated by documenting the breadth of its application as found in the refereed literature, a direct comparison with measured wave height data for two historic hurricanes in the region and a comparison of wave-setup predictions with two other models. The model was tested on three validation runs and implemented in 228 production runs for different hurricanes striking the Mississippi Coast.

Additional References

Komen, G.J., Cavaleri, L., Donelan, M., Hasselmann, K., Hasselmann, S., Janssen, P.A.E.M. 1994, Dynamics and Modelling of Ocean Waves, Cambridge University Press, Cambridge, 532 pages.

Dean, R. G. and Bender, C. J., Static Wave setup with emphasis on damping effects by vegetation and bottom friction, Coastal Engineering, 2006, 53, 149-156.

Sheppard, D. M., Slinn, D. N., Hagen, S., 2007, Design Hurricane Storm Surge Study, Final Report, Florida Department of Transportation. 149 pgs.

Shore Protection Manual, 1984, 4th Edition, 2 Volumes, USACE, US Army Coastal Engineering Research Center, US Government Printing Office, Washington, D.C., 1,088 pgs.

Coastal Engineering Manual, 2002, US Army Corps of Engineers, EM 1110-2-1100, Vicksburg, Mississippi.

Appendix A: Whafis Offshore Boundary Conditions for the Transect Table

Transect	Longitude	Latitude	100 Year Height	100 Year Period	500 Year Height	500 Year Period
1	-88.74884	30.34119	1.813701	4.388661	2.22262	5.081293
2	-88.39566	30.383627	1.69083	4.240767	2.149277	5.209322
3	-88.409714	30.341639	1.580183	5.302158	2.026063	5.905477
4	-88.422119	30.35413	1.65504	4.324093	2.106221	4.987391
5	-88.436752	30.356781	1.500166	4.226223	1.948354	4.993164
6	-88.446938	30.337177	1.427027	5.083234	1.86148	5.356519
7	-88.464859	30.324638	1.48792	5.22294	1.912359	5.419188
8	-88.478615	30.318497	1.39512	4.826024	1.811334	5.648623
9	-88.486221	30.318926	1.394397	5.132036	1.81072	5.86076
10	-88.493767	30.319384	1.464812	5.304868	1.877141	6.063148
11	-88.501076	30.320093	1.400319	5.20028	1.816239	6.086147
12	-88.517799	30.334332	1.014038	1.672328	1.99028	4.941429
13	-88.523949	30.340439	1.444314	4.540401	1.903279	5.664071
14	-88.531601	30.34222	1.506092	4.756896	2.012298	5.944237
15	-88.535507	30.343082	1.582242	4.752531	2.004215	5.619851
16	-88.540131	30.343693	1.355302	4.656222	1.970682	6.274804
17	-88.547279	30.343439	1.52041	4.724558	1.95538	5.576342
18	-88.553314	30.343239	1.555868	4.692284	1.996775	5.476469
19	-88.560135	30.343557	1.483797	4.625305	1.974333	5.633997
20	-88.576332	30.328094	1.994108	4.553117	2.379382	5.310725
21	-88.58651	30.340801	1.813419	3.931597	2.242095	4.542615
22	-88.591721	30.360365	1.508137	3.604015	1.8475	4.261131
23	-88.602379	30.36908	1.566069	3.717484	1.88099	4.318422
24	-88.604691	30.375475	1.407183	3.737863	1.804708	4.336937
25	-88.607025	30.376245	1.376074	3.433163	1.706518	3.972538
26	-88.617348	30.372589	1.213384	3.832535	1.963483	4.56963
27	-88.623856	30.368729	1.469904	4.001294	1.949027	4.749401
28	-88.630814	30.365545	1.625953	3.950252	2.07937	4.644265
29	-88.639084	30.359449	1.603711	3.940125	2.051767	4.556791
30	-88.646942	30.359694	1.515813	4.031947	1.973463	4.644318
31	-88.652802	30.359926	1.526286	4.166439	1.985641	4.725777
32	-88.662575	30.361816	1.459955	4.224504	2.076738	5.301245
33	-88.672142	30.359034	1.519226	4.367541	1.992636	5.064579
34	-88.681282	30.354195	1.575049	5.069269	2.049333	5.415625
35	-88.696075	30.34535	1.507238	5.215951	1.992526	5.66028
36	-88.712921	30.342278	1.505738	5.002498	1.993935	5.457777
37	-88.7314	30.342968	1.498099	4.552695	1.977836	5.392147
38	-88.75251	30.351513	1.500569	4.127944	1.965787	5.268389
39	-88.764297	30.360363	1.433148	4.121272	1.931057	5.401195
40	-88.770424	30.36438	1.5095	4.274673	1.981296	5.377168
41	-88.776817	30.368097	1.575142	4.470894	2.026615	5.467354
42	-88.783592	30.371286	1.630371	4.399496	2.105528	5.569633
43	-88.790703	30.374243	1.648696	4.322258	2.139354	5.535193
44	-88.797409	30.377785	1.686207	4.156553	2.165856	5.37672

Transect	Longitude	Latitude	100 Year Height	100 Year Period	500 Year Height	500 Year Period
45	-88.804291	30.381182	1.657025	4.765151	2.145249	5.285723
46	-88.811638	30.384792	1.699643	4.656991	2.195144	5.227871
47	-88.815361	30.397858	1.640239	4.605323	2.10857	5.208837
48	-88.837975	30.369375	1.787696	4.866464	2.334666	5.617022
49	-88.846237	30.372976	1.79204	4.9153	2.38482	5.795378
50	-88.853096	30.376143	1.795182	4.825648	2.403769	5.795266
51	-88.856239	30.377523	1.805961	4.746658	2.326157	5.712741
52	-88.858032	30.430401	1.469209	4.026794	1.967346	5.225512
53	-88.863586	30.427912	1.61073	3.913695	2.137547	5.46469
54	-88.869469	30.428848	1.502456	3.976819	2.001228	5.162845
55	-88.874886	30.423645	1.546983	3.950918	1.972936	4.828823
56	-89.348557	30.370842	2.085191	4.709369	2.646759	5.449972
57	-89.353958	30.368055	2.073405	4.553126	2.629421	5.366238
58	-89.358894	30.36268	2.037271	4.357728	2.600871	5.218809
59	-89.362907	30.359524	2.014829	4.216673	2.578289	5.273904
60	-89.366806	30.352215	2.051982	4.186459	2.56986	4.909026
61	-89.36599	30.346066	2.083079	4.158914	2.556767	4.683887
62	-89.332123	30.335623	1.849398	5.001392	2.462238	5.857585
63	-89.325691	30.322756	1.557392	5.17316	2.935276	6.32633
64	-89.322517	30.313177	2.396127	5.41342	3.048962	6.406531
65	-89.325768	30.308395	2.349226	5.553821	3.026252	6.579685
66	-89.329659	30.302273	2.442226	5.668756	3.116326	6.532453
67	-89.335297	30.297421	2.427088	5.5012	3.103038	6.504386
68	-89.34169	30.293348	2.396524	5.630061	3.135792	6.527155
69	-89.349258	30.290901	2.432819	5.638608	3.118512	6.453191
70	-89.357132	30.289059	2.37296	5.550907	3.040466	6.408204
71	-89.364052	30.285248	2.359902	5.75944	3.118716	6.743686
72	-89.369476	30.280855	2.451166	5.545288	3.194136	6.632535
73	-89.373947	30.274912	2.505045	5.577464	3.174076	6.492041
74	-89.379517	30.270197	2.456051	5.586907	3.196485	6.532156
75	-89.386169	30.266495	2.476571	5.603651	3.148959	6.478945
76	-89.393112	30.263241	2.56449	5.928434	3.22793	6.55671
77	-89.401413	30.261839	2.30981	6.117692	3.072522	7.103522
78	-89.408607	30.259327	2.392177	5.933012	3.035865	6.577899
79	-89.415413	30.256231	2.397825	5.888074	3.059161	6.623128
80	-89.420654	30.252491	2.403683	5.832417	3.03758	6.447159
81	-89.424194	30.246504	2.342455	6.122664	3.043019	6.956621
82	-89.424805	30.241684	2.386446	5.982381	3.083243	6.692477
83	-89.435867	30.214802	2.775491	5.511075	3.348581	6.225808
84	-89.446327	30.205469	2.481176	5.730548	3.10729	6.382622
85	-89.449814	30.183939	2.632483	5.818463	3.27437	6.474339
86	-89.478188	30.192665	2.668324	5.007576	3.342026	6.092613
87	-89.49073	30.186932	2.471221	5.221769	3.125877	6.476115
88	-89.501671	30.182459	2.64393	5.274992	3.229737	6.192059
89	-89.51915	30.18329	2.720707	5.334184	3.31766	6.155225
90	-89.531021	30.185715	2.372704	5.605432	2.953512	6.085907
91	-89.548019	30.182199	2.467733	5.0439	3.038692	5.948472

Transect	Longitude	Latitude	100 Year Height	100 Year Period	500 Year Height	500 Year Period
92	-89.561363	30.178051	2.819999	5.282553	3.379086	5.739
93	-89.569771	30.172579	2.648313	5.051359	3.24087	5.799189
94	-88.858574	30.403421	1.031202	4.848148	1.644691	5.80023
95	-88.857643	30.393654	1.182556	4.643119	1.692304	5.502983
96	-88.86216	30.380384	1.891444	4.561799	2.435438	5.34115
97	-88.869934	30.383541	1.901337	4.524246	2.484504	5.329502
98	-88.871849	30.391863	1.770541	4.595313	2.276756	5.495105
99	-88.87986	30.392776	1.870407	4.699517	2.356335	5.40141
100	-88.888657	30.391302	2.036257	4.605489	2.589861	5.541136
101	-88.897057	30.39345	1.805664	5.16589	2.339997	5.999481
102	-88.902618	30.393671	1.811878	5.329814	2.402006	6.174042
103	-88.910538	30.393805	1.816569	5.235875	2.365527	6.199424
104	-88.918434	30.393791	1.831817	5.394998	2.390843	6.311996
105	-88.9263	30.393303	1.923577	5.293822	2.482466	6.176072
106	-88.934158	30.392399	1.875623	5.279471	2.436713	6.117637
107	-88.942062	30.39225	1.835833	5.273961	2.393474	6.098217
108	-88.949966	30.391804	1.808627	5.319631	2.370108	6.097491
109	-88.957886	30.391483	1.885305	5.364504	2.479195	6.131922
110	-88.965797	30.391006	1.879614	5.429115	2.503189	6.144783
111	-88.973686	30.390442	1.941754	5.598406	2.504673	6.338859
112	-88.981453	30.389076	1.932831	5.639641	2.561534	6.424379
113	-88.989342	30.388412	2.003701	5.713234	2.582675	6.533176
114	-88.997131	30.387289	1.946669	5.722618	2.62724	6.549475
115	-89.004936	30.386175	1.992137	5.752616	2.579507	6.572398
116	-89.01268	30.384701	2.013543	5.872194	2.667888	6.498242
117	-89.02037	30.382999	1.997365	5.86598	2.654279	6.532282
118	-89.027946	30.380968	1.995234	5.916663	2.661211	6.633861
119	-89.035629	30.3794	2.000595	5.736152	2.667654	6.481209
120	-89.04319	30.377752	2.014418	5.764431	2.678429	6.595845
121	-89.050629	30.376093	1.99349	5.800861	2.676809	6.596533
122	-89.058182	30.374315	2.01103	5.412256	2.682451	6.61404
123	-89.065956	30.373095	2.009075	5.482696	2.704667	6.728029
124	-89.073448	30.370842	1.975739	5.467371	2.600574	6.696744
125	-89.080994	30.368727	1.850466	5.813518	2.478631	6.729534
126	-89.08493	30.361315	2.348587	5.832418	2.967017	6.632874
127	-89.093605	30.360971	1.801545	5.218595	2.43389	6.086803
128	-89.102859	30.361235	1.908191	5.220904	2.583356	6.257352
129	-89.110031	30.358309	1.989309	5.602091	2.702199	6.545395
130	-89.117271	30.355616	1.9806	5.595172	2.697713	6.408088
131	-89.124878	30.354132	1.951099	5.572067	2.695271	6.695927
132	-89.131958	30.351053	2.079934	5.664422	2.7572	6.744116
133	-89.139053	30.347549	2.04963	5.828616	2.687959	6.68629
134	-89.14592	30.344746	2.118087	5.524574	2.777272	6.819166
135	-89.153488	30.342703	2.06974	5.556586	2.79439	6.617477
136	-89.160774	30.340021	1.967798	5.413367	2.692189	6.58427
137	-89.168198	30.337597	2.086082	5.462409	2.790476	6.680572
138	-89.175468	30.334883	2.134661	5.393308	2.822163	6.864919

Transect	Longitude	Latitude	100 Year Height	100 Year Period	500 Year Height	500 Year Period
139	-89.182663	30.332026	2.156438	5.441752	2.896631	6.690437
140	-89.190376	30.330481	2.158976	5.357239	2.938012	6.83175
141	-89.197975	30.328535	2.141661	5.237891	2.927989	6.870198
142	-89.205536	30.326494	2.290321	5.965293	2.989494	6.765438
143	-89.213188	30.324959	2.321004	5.997658	3.016631	6.782957
144	-89.220718	30.322515	2.247957	5.994801	2.938671	6.756035
145	-89.227913	30.319626	2.3134	6.037979	3.009139	6.761075
146	-89.235191	30.316925	2.335835	5.962182	3.036344	6.692785
147	-89.242561	30.314449	2.327209	5.867947	3.098345	6.607321
148	-89.25074	30.311993	2.231414	5.749161	3.026667	6.95932
149	-89.257347	30.310312	2.21536	5.637394	3.001819	6.972602
150	-89.264717	30.307817	2.385662	5.551509	3.077725	6.597131
151	-89.272141	30.305428	2.348063	5.675549	3.115702	6.636679
152	-89.279846	30.303841	2.385859	5.650869	3.14546	6.666057
153	-89.287712	30.303164	2.504955	5.601517	3.167217	6.607004
154	-89.293571	30.306124	2.401897	5.375008	3.036514	6.415527
155	-89.276321	30.347385	1.763361	4.279789	2.200192	4.475662
156	-89.288223	30.361082	1.920085	4.1839	2.399233	4.878481
157	-89.293541	30.365829	1.93461	4.457421	2.453343	5.003556
158	-89.30014	30.366398	2.000131	4.251539	2.534379	5.103378
159	-89.312218	30.374662	2.094347	4.382735	2.620264	5.357765
160	-89.319763	30.374765	2.074986	4.510056	2.601256	5.429707
161	-89.333397	30.373926	2.133271	4.861291	2.648122	5.612226